nature portfolio

Peer Review File

Submolecular video-imaging of the Smc5/6 complex topologically bound to DNA

Corresponding Author: Dr Kenichi Umeda

This file contains all reviewer reports in order by version, followed by all author rebuttals in order by version.

Version 0:

Reviewer comments:

Reviewer #1

(Remarks to the Author)
In the submitted manuscript, the authors adopt high-speed atomic force microscopy to visualise the dynamics of the Smc5/6 complex in isolation and on DNA.

They found that Smc5/6 in isolation adopted two conformations: an “I”-shaped conformation with two closely aligned SMC arms and an “O”-shaped open-ring conformation. They also show that ATP is required to transition from the I-shaped to the O-shaped ring conformation by both ensemble mutant analysis, simulations and HS-AFM tracking.

They show that by adopting a supported lipid bilayer, it is possible to visualise different states of the Smc5/6 complex bound to DNA. The analysis of such datasets revealed that the Smc5/6 complex can bind DNA in two alternative ways: through association to the DNA at the hinge domain (either in I or O conformation) or through the ATPase head (mainly in the I conformation), ATP hydrolysis being necessary to establish the Hinge—DNA binding.

Finally, they show that the Smc5/6 complex mediates DNA compaction, potentially through DNA twisting.

Overall, the manuscript is of very high quality, and the data very convincingly support the conclusions, and I recommend publication pending some clarifications/modifications.

Specifically: the quantifications are clearly described, albeit some seem to be strongly dependent on human-based curation and should be either automatised or described more in detail. If some discrectionality is involved, an independent analysis from at least another independent evaluator should be conducted to assure robustness. Specifically:

• For the analysis presented in Figure1: “We quantified the occurrence frequencies of these two structures based on the conformations observed within the initial ten frames after the molecules appeared in 7 / 56 the AFM images.”
Which objective criteria can be used to assign the images to specific classes?
Would two independent evaluators always produce the same assignment?
Same question for Figure 5e.
• For the analysis in Figure 3: How was the central position for each molecule from where the angles were then calculated determined? If manually, how robust is the angle determination to small variations in the central point determination?
• For the analysis in Figure 6, where were the points on the DNA for the contour placed, where the complex was overlaid to the DNA itself? How robust is the analysis to such a placement?

Finally, in the material and methods, it is stated that:

“To quantitatively measure the molecular size and DNA length, we implemented a function to compensate for the nonlinearity and tip-position dependence of the XY piezo scanner (this will be published elsewhere)”

Such a statement makes it hard to evaluate the appropriateness of the procedure (likely correct given the expertise of the authors, but still unverifiable at this point). Perhaps the author could explain the concept behind it without going into too much detail or, vice versa, briefly show any data in support of the correctness without revealing details?

Reviewer #2

(Remarks to the Author)
In this study, the authors used high-speed atomic force microscopy (HS-AFM) to visualise the structural dynamics of budding yeast Smc5/6 complexes at submolecular resolution. Within the Smc5/6 hexamer, they predominantly observed two types of extended architectures—the I-form and the O-form—whose prevalence correlated with the ATP-binding state of the complex. They also found that Nse2 stabilises the extended conformation of Smc5/6 by preventing elbow bending within the SMC arms, in contrast to the flexible elbow dynamics characteristic of cohesin and condensin. Based on these findings, the authors propose that Smc5/6 compacts DNA through a DNA–DNA tethering mechanism. More broadly, they suggest that DNA–DNA tethering may be a conserved biochemical property among SMC complexes, complementing their ability to extrude DNA loops. The manuscript is well written and easy to follow. I The resolution the authors achieved in their HS-AFM experiments is impressive. Overall, Ithis work adds valuable insights to research on SMC complex activities.

Comments:

Nse2 dissociation
My main concern relates to the interpretation of Nse2 dissociation. I am not entirely convinced that the results presented in this section (Fig. 3, Supplementary Fig. 4, and Supplementary Movie 3) sufficiently support such a strong conclusion. I would recommend validating the proposed complex dynamics by performing additional biophysical experiments specifically examining Nse2 association and dissociation.

Lines 278-280
Did authors try to carry out this experiment with the wt Smc5/6 and ATP analogues? Especially in the context of experiment of DNA recovery (Fig. 6e).

LINE 101:
Does DNA binding shift the equilibrium toward the O-form? Given that DNA has been shown to stimulate ATP hydrolysis, it would be valuable to assess whether it also stabilizes the “O-form,” in which the ATPase heads of SMC5/6 are engaged. This could potentially be tested using a short dsDNA oligonucleotide, similar to the approach used for the cryo-EM structure of SMC5/6 bound to DNA. It may additionally be informative to test oligos containing an ss/ds junction, to examine SMC5/6 conformations relevant to structures arising during replication stress or double-strand break repair.

LINE 167:
For SMC5, the center of mass of the Nse2 subunit could reasonably be used to define a point for angle measurement along the coiled coil. For SMC6, however, this is more difficult as there is no equivalent density at the coil midpoint. Because the angle determination is based on manually selected points rather than a statistical framework (as stated in the Methods, Line 780: “three control points were manually placed”), I would caution against reporting numerical angle values, as they may appear somewhat arbitrary.

LINE 171:
The final step shown in Figure 3d is described as a “broken” complex with a split hinge; however, in both the figure and Supplementary Movie 3, it is hard to discriminate 2 hinge domains. Could the final step of figure 3d be interpreted as an “I-form” without the Nse2 subunit?
Additional observations could be made on Supplementary Movie 3. For example, in the frames 16.4s – 16.7s -17s there seems to be a rapid detachment of the ATPase heads, followed by a rebinding. After that the conformation of the of the complex results less clear.
To support the interpretation of the proposed “B-structure” or “broken complex,” it would strengthen the manuscript if additional representative examples were included.

LINE 184:
The linear DNA retention data (Fig. S5a) suggest that the EQ mutant may in fact retain DNA more effectively than the WT protein. Maybe this could reflect DNA binding in the clamp conformation, without transition in other regions of the SMC5/6 complex. This seems to be confirmed in Supplementary movie S4 and S5. In movie S4, the WT protein seem to interact with the DNA at the hinge domain, (probably after a first entrapment of the DNA between the heads) and seems to be jumping around the DNA quite often (second 50.9, second 105.8), which explains why upon linearization the DNA is lost. Instead, the EQ mutant is stuck in one position, and the DNA is entrapped between the heads domain in the clamp conformation. Could the authors elaborate the discussion considering these points?

SUPPLEMENTARY FIGURE 7a:
It would be informative if the authors could measure the head–hinge distances in the four displayed snapshots and comment on whether this correlates with the proposed conformational states.
More generally, the first two images classified as Head-I may also be explainable as Head-O viewed with the O-ring oriented perpendicular rather than parallel to the imaging plane. Similar considerations could apply to Figure 5b–c.

LINE 317: “We speculate that Smc5/6 initially entraps DNA within the kleisin compartment and subsequently transfers it to the SMC compartment upon ATP hydrolysis”
The authors propose that DNA is initially captured inside the kleisin compartment and later transferred into the SMC

compartment upon ATP hydrolysis. However, available cryo-EM structures of SMC complexes—including SMC5/6 (Yu et al., PNAS, 2022)—show DNA occupying the SMC compartment even in ATP-engaged but hydrolysis-defective states. While AFM clearly demonstrates Head-O binding near the ATPase domains, it remains unclear whether the DNA lies inside or outside the SMC ring.
A potential experiment to test this model would be to pre-engage the heads using the SMC5/6 EQ mutant with ATP or ADP-BeF_3, then introduce DNA afterward and visualize using AFM. If the DNA can be captured by a pre-closed complex, it may indeed indicate initial kleisin-only entrapment.

Minor comments:

Line 132: Fig.2e in red.
Lines 221-222 : The sentence is not clear. Please restructure it to improve readability.
Lines 290-292 :I suggest explicitly highlighting that DNA-tethering activity requires ATP binding but not ATP hydrolysis.
Line 299 :The word mediate is used twice ("…Smc5/6 mediates mediate DNA–DNA tethering…").

Reviewer #3

(Remarks to the Author)
In this manuscript, the authors use high-speed AFM (HS-AFM) to visualise budding yeast Smc5/6. They present data showing two conformations for the Smc5/6 hexamer, characterised by I- and O-shaped complexes and track transitions between these two states demonstrating through the use of an ATP hydrolysis mutant (EQ) that ATP binding causes the transition to O shape. They also investigate the ability of Smc5/6 to engage DNA and classify interactions based on whether they occur through different regions of the complex (i.e. heads and hinge). The authors argue that these interactions represent different stages of topological loading, meaning that the DNA is caught within the SMC-kleisin tripartite architecture. They used biochemical bulk assays that include high salt washes as a main argument for topological loading. Finally, they also propose DNA:DNA tethering by Smc5/6 and DNA compaction, using a combination of AFM and bulk assays.
The technical execution of AFM and the image quality are very good, and the lipid-supported system is a valuable advance. The authors clearly observed the predicted structure of Smc5/6 and demonstrate the I and O states and convincingly link the ATP binding in the transition between the two states. They also show that on DNA SMC head regions readily interact with DNA upon ATP binding, using the EQ complex.
However, they argue that they are observing topological loading on DNA, making this point a key claim of their work. Unfortunately, this topological binding is not supported by the data. In fact the AFM data strongly argues against it.
In summary, although the HS-AFM imaging is of high technical quality and the conformational transitions between I and O states are convincingly documented, the manuscript ultimately demonstrates only that Smc5/6 interacts with DNA mainly through its ATP-head regions upon ATP binding, an interaction already well supported by prior structural work. The central claim that these observations represent topological loading is not backed by the data presented, and several aspects instead argue against such an interpretation. As a result, the manuscript risks introducing misconceptions into the field rather than clarifying Smc5/6 mechanism. I cannot support publication of this work unless the authors unequivocally demonstrate, through appropriate crosslinking-based assays, that the complexes they visualise are indeed topologically loaded.

Specific comments
1. One of the central claims of the manuscript is that Smc5/6 topologically loads onto DNA and that HS-AFM directly visualises this binding with DNA within either the kleisin or SMC compartments. Salt-resistant binding does not necessarily imply topological entrapment. The authors rely heavily on high-salt washes (Fig. 4b) to infer topological capture. Numerous studies on cohesin have shown that salt resistance alone is insufficient to distinguish between topological and strong non-topological binding, for example when DNA is in the gripping state (not topologically loaded). Importantly, topological entrapment has been demonstrated in previous studies through crosslinking of the interfaces of the SMC-kleisin tripartite ring, something that is not done here. Crosslinking experiments demonstrated that topological entrapment is strongly driven by ATP-hydrolysis. In contrast, DNA interactions that survive high-salt washes can still occur in the absence of ATP hydrolysis. Here the authors show that their EQ hydrolysis mutant resists high-salt washes therefore in this experimental conditions the authors cannot conclude that topological loading has been achieved.
In addition, the AFM data clearly contradicts topological entrapment. The authours show that wild-type complexes freely transition between I and O conformations and they argue that are these complexes are topologically loaded in their AFM images, however the complexes can be observed in the movies to jump from one side of the DNA to another, something impossible if DNA were threaded inside a closed ring. Please refer to Movie S4 and S6 (left pannel for WT complexes; loaded complexes detach and reattach at distal/different positions along the DNA contour).
There is also a degree of confusion when interpretating of the imaging data. In Fig. 4e the authors state that Smc5/6 is engaged with DNA through a hinge-mediated, topologically trapped intermediate. However, the still image they present in this figure corresponds to a frame from Movie S4, and the full movie shows a completely different behaviour: again the complex argued to be topologically loaded seems to jump from one side of the DNA to the other in a single frame during the movie. Such a discontinuous relocation is incompatible with any form of topological entrapment. Similar situation is shown in Fig. 5b, and Movie S6.
In addition, the authors overinterpret the meaning of small linear movement of the complex along DNA, claiming that it is evidence for a topologically entrapped state. Linear displacement on DNA can also arise from simple one-dimensional diffusion of a protein bound non-topologically, particularly under the high-salt conditions used in the assay where

electrostatic screening reduces non-specific sticking and facilitates sliding. Diffusive motion therefore cannot be taken as an indicator of ring-closure or topological capture.
The manuscript does not provide adequate biochemical or AFM evidence to support its central claim of topological loading. Definitive assignment of DNA to either the kleisin or SMC compartment requires conditional closure of specific ring interfaces by crosslinking. Cross-linking of the Smc–kleisin interfaces has long been the gold-standard biochemical test for topological entrapment, and including these experiments here would allow the authors to distinguish unequivocally between topological and non-topological associations. Without such controls, the current data remain insufficient to sustain the claims made.
2. A further concern relates to the authors' claim of DNA:DNA tethering activity based on AFM data. The events they interpret as "tethering" appear to be extremely transient, often limited to a single or a few frames, and, as presented, are indistinguishable from stochastic contacts between two nearby DNA segments containing complexes. Short-lived proximity or brief co-movement is not sufficient evidence of a genuinely stable bridging interaction, particularly in an AFM setting.
To substantiate a tethering mechanism, the authors would need to demonstrate persistent and mechanically meaningful interactions events that remain stable across multiple frames or show coordinated movement of both DNA arms in a way that cannot be explained by random diffusion. Without such evidence, the interpretation of these very brief contacts as "tethers" is not convincing.

Other comments
1. It is well-established that Smc5/6 hinge has a preference for ssDNA rather than dsDNA. The authors mention that Smc5/6 associates strongly with nicked plasmids. Since a nicked plasmid, even if mostly double-stranded, inevitably carries local ssDNA regions, could these intereactions represent engagement with ssDNA?.
2. The authors need to compare the behaviour of hexameric versus octameric Smc5/6 assemblies on DNA by AFM and contrast their binding behavior. Nse5/6 is required for bona fide topological loading, and therefore any claim of topological entrapment made from octamer-based assays must be contrasted with the behaviour of the hexameric core. Such a comparison may reveal mechanistic differences that could be attributed to conditions where topological binding can (or cannot) occur.

Version 1:

Reviewer comments:

Reviewer #1

(Remarks to the Author)
I thank the authors for their thorough revisions and responses to my comments. The authors have satisfactorily addressed all of my concerns, including those related to the robustness and description of the quantitative analyses.

The manuscript provides valuable insights into the conformational dynamics of the Smc5/6 complex and its interactions with DNA through high-speed AFM. The study advances our understanding of ATP-dependent conformational changes, alternative DNA-binding modes, and DNA compaction by Smc5/6.

I am satisfied with the revised manuscript and consider it suitable for publication in its current form.

(Remarks on code availability)

Reviewer #2

(Remarks to the Author)
the authors have clarified the issues raised in the previous version of the manuscript and improved the clarity of the manuscript

(Remarks on code availability)

Reviewer #3

(Remarks to the Author)
I thank the authors for their thorough and carefully considered response to my concerns. The additional experiments have strengthened the manuscript in several important respects, and I acknowledge the significant effort made to address my criticisms. However, I maintain several reservations that I outline below.

Topological loading, Nse5/6 dependency
The new data demonstrating that the Smc5/6 hexamer lacking Nse5–Nse6 fails to load onto DNA in both bulk assays and HS-AFM imaging (0 of 76 DNA molecules bound) is the most convincing addition to the manuscript. Since Nse5–Nse6 dependence is an established hallmark of topological loading, this result substantially strengthens the authors'

interpretation. I am largely satisfied by this response, and consider this the most important advance over the original submission.

Jumping behaviour and apparent dissociation/re-association
The authors' explanation, that apparent jumping events reflect transient detachment of DNA from the lipid membrane followed by rapid lateral diffusion within a single frame acquisition time is plausible. The supporting experiment showing that freely diffusing Smc5/6 in the imaging buffer cannot bind to pre-adsorbed DNA further argues against simple rebinding as an explanation for these events. I accept that the authors have provided a reasonable account of the jumping artefact. However, I note that this explanation was developed post hoc in response to my criticism, and the evidence for it remains indirect. The authors infer that DNA briefly lifts off the membrane based on apparent distortion of the DNA contour during jump events, which is suggestive but not conclusive. A more direct demonstration (for example by systematically varying lipid membrane composition to modulate DNA adsorption strength and showing that jump frequency correlates accordingly) would have been more convincing. I acknowledge this may be beyond the scope of the current revision, and I do not insist on it as a condition for publication, but I would ask the authors to present this explanation clearly as an inference rather than an established fact in the revised manuscript.

Crosslinking-based ring closure assays
I appreciate the authors' position that compartment-specific crosslinking experiments address a conceptually different question from what their HS-AFM study examines. Nevertheless, I remain of the view that making a strong claim of topological entrapment without the gold-standard biochemical validation leaves the manuscript vulnerable. The Nse5/6 dependency data provides important indirect support, but it demonstrates a requirement for a factor known to be involved in topological loading, not topological loading itself. I will not insist on crosslinking experiments as an absolute condition for publication given the new supporting data. However, I strongly urge the authors to explicitly acknowledge in the Discussion that direct biochemical proof of ring closure (through interface-specific crosslinking) has not been performed in this study, and that their interpretation of topological loading is based on convergent indirect evidence. This is an honest and important qualification that readers deserve, and it is consistent with rigorous scientific reporting.

DNA-DNA tethering
The new data showing that over 80% of twisted species bound by multiple Smc5/6 molecules maintain stable DNA-DNA tethering over 60–120 consecutive frames (1–2 minutes) substantially addresses my concern about the transient nature of the observed bridging events. The examples of coordinated movement of two DNA strands with apparent loop formation are also more convincing than what was presented originally. I am satisfied that this claim is now better supported, though I note that the mechanistic interpretation of how Smc5/6 mediates this tethering (whether through simultaneous engagement of two DNA segments by a single ring or through oligomerisation) remains speculative and should be presented as such.

In summary, the authors have made meaningful progress in addressing my concerns. The Nse5/6 dependency experiments represent a genuine advance and substantially shift the evidential basis for topological loading. The remaining gap (absence of direct crosslinking-based ring closure evidence) should be acknowledged explicitly as a limitation rather than left implicit. Subject to this acknowledgement being incorporated clearly into the Discussion, and to the jumping artefact explanation being presented as an inference rather than a conclusion, I am prepared to support publication.

(Remarks on code availability)

Point-by-point response to Reviewers' comments

We would like to thank the three reviewers for their interest in our study and for their constructive and critical comments. We have performed additional experiments in response to their suggestions, and we hope the reviewers will agree that the revised manuscript has been improved and that our conclusions have been strengthened. A point-by-point response to all comments is provided below. Reviewer comments are shown in blue, followed by our responses in black. The revised sentences in the main text, updated according to the new results, are highlighted in light blue.

Response to Reviewer #1: In the submitted manuscript, the authors adopt high-speed atomic force microscopy to visualise the dynamics of the Smc5/6 complex in isolation and on DNA. They found that Smc5/6 in isolation adopted two conformations: an "I"-shaped conformation with two closely aligned SMC arms and an "O"-shaped open-ring conformation. They also show that ATP is required to transition from the I-shaped to the O-shaped ring conformation by both ensemble mutant analysis, simulations and HS-AFM tracking. They show that by adopting a supported lipid bilayer, it is possible to visualise different states of the Smc5/6 complex bound to DNA. The analysis of such datasets revealed that the Smc5/6 complex can bind DNA in two alternative ways: through association to the DNA at the hinge domain (either in I or O conformation) or through the ATPase head (mainly in the I conformation), ATP hydrolysis being necessary to establish the Hinge—DNA binding. Finally, they show that the Smc5/6 complex mediates DNA compaction, potentially through DNA twisting. Overall, the manuscript is of very high quality, and the data very convincingly support the conclusions, and I recommend publication pending some clarifications/modifications.

Specifically: the quantifications are clearly described, albeit some seem to be strongly dependent on human-based curation and should be either automatised or described more in detail. If some discrectionality is involved, an independent analysis from at least another independent evaluator should be conducted to assure robustness.

General comments:

We thank Reviewer 1 for their positive comments on our study and for recognizing its significance. Reviewer 1 raised several important points regarding the robustness of the quantification of Smc5/6 molecules, the determination of SMC arm angles, and the quantification of DNA-bound Smc5/6 molecules. To address these concerns, we have added detailed descriptions of these analyses to the main text together with the corresponding supplementary figures. In addition to the first author, three independent analysts (co-authors of this study) analyzed the same representative datasets to assess the reproducibility of the measurements. We also performed a theoretical estimation of the error associated with SMC arm-angle determination. These additional analyses, conducted in response to Reviewer 1's suggestions, further support the conclusions of our study.

• For the analysis presented in Figure1: "We quantified the occurrence frequencies of these two structures based on the conformations observed within the initial ten frames after the molecules appeared in the

AFM images." Which objective criteria can be used to assign the images to specific classes? Would two independent evaluators always produce the same assignment? Same question for Figure 5e.

Thank you for this insightful comment. In Fig. 1, I- and O-forms were classified based on whether the mica surface was exposed between the two SMC arms: exposure indicated the O-form, whereas no exposure indicated the I-form. As shown in Response Fig. 1, the line profiles clearly distinguish these states, with a substrate-level minimum (mica surface) observed between the arms in the O-form but absent in the I-form (this data is now shown in new Supplementary Fig. 2a).

For the classification of DNA-bound Smc5/6 on the lipid membrane in Fig. 5e, we first identified SMC-shaped molecules based on the structures observed in Fig. 1. We then identified the two globular domains in each molecule, assigning the larger one as the head domain and the smaller one as the hinge domain. We further classified particles according to whether the head or hinge domain was bound to DNA, defining head-binding and hinge-binding modes. Using the same criteria as in the mica experiments, the head-binding mode was further divided into Head-O and Head-I forms.

To assess the robustness of the molecular classification shown in Figs. 1d and 5e, four independent evaluators (authors of this study) performed the classification independently. Representative datasets were analysed under three conditions: WT molecules on mica, DNA-bound WT on lipid membranes, and DNA-bound EQ mutant on lipid membranes, and inter-annotator agreement was evaluated. As a result, >95% agreement was achieved with 100% concordance for all conditions, demonstrating high robustness (Response Fig. 1c). These data have been added to Supplementary Fig. 1b.

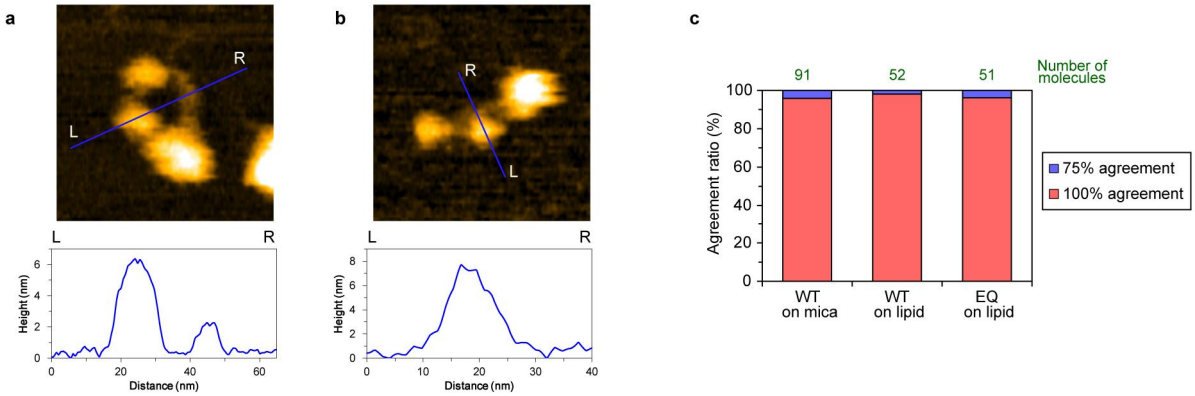

Umeda_et_al_Response_Fig.1

Response Figure 1| Classification of O-form and I-forms

a,b, Representative HS-AFM images of the O-form (a) and I-form (b) (upper), and the corresponding line-profile analyses drawn across the Smc5 and Smc6 arms (lower). Line profiles showed a presence of a substrate-level minimum (i.e. mica surface) between the SMC arms in the O-form, which was absent in the I-form.

c, Statistical evaluation of the classification agreement for WT molecules observed on mica (analysis of Fig. 1d), and the DNA-bound WT and EQ mutant molecules using the lipid membrane stage (analysis of Fig. 5e). Four independent analysts performed the classification, and agreement rates exceeding 95% were obtained under all conditions, demonstrating the robustness of the classification procedure.

• For the analysis in Figure 3: How was the central position for each molecule from where the angles were then calculated determined? If manually, how robust is the angle determination to small variations in the central point determination?

Thank you for this insightful comment. We manually drew two straight lines along each SMC arm in each frame to determine the elbow angle. For Smc5, three control points were placed at the head, hinge, and Nse2 positions, and these points were used to define two straight segments, from which the intersection angle was calculated. For Smc6, two control points were placed at the head and hinge. The third control point was placed on the curved region of its arm. As shown in Fig. 2, our simulation showed that the O-form conformation can be induced by bending the Smc6 arm at the Joint 1 elbow, which is located at a 40:60 ratio relative to the hinge-elbow and elbow-head. We placed the control points according to this ratio. In some frames, the Smc6 arm appeared straight, and the curvature of the arm was not clearly visible. In such cases, we positioned the control point on the SMC6 arm at a ratio of 40:60 relative to the hinge-elbow and elbow-head joints.

When the arm length is sufficiently large compared with its widths, the defined angle is uniquely determined. In actual HS-AFM images, however, the finite arm widths, measurement noise, and slight asymmetry of the cross-sectional height profile can introduce some uncertainty in the placement of control points. Below, we therefore provide a theoretical estimate of the angular error arising from these factors (Response Fig. 2).

The arm length of Smc5 and Smc6 is approximately 30 nm, and the elbows are estimated to located at 43:57 for Smc5 and 40:60 ratio for Smc6 relative to the hinge-elbow and elbow-head, respectively, based on our molecular simulation shown in Fig. 2. Thus, as illustrated in Response Fig. 2a, we approximate the lines connecting the hinge–elbow–head points as forming a scalene triangle. If the total arm length is denoted by L_0, the lengths of the two segments, L_1 (hinge–elbow) and L_2 (elbow–head), are expressed as follows.

$$\begin{aligned} L_1 &= \alpha L_0, \\ L_2 &= (1-\alpha) L_0, \end{aligned} \tag{1}$$

where α represents the relative position of the elbow along the arm, corresponding to values of α=0.43 and α=0.40 for Smc5 and Smc6 arms, respectively.

At this point α, we define the base lengths as a_1 and a_2, and the height as h_0. If the apex angle, divided by the two sides L_1 and L_2, is denoted by ϕ_0, and the two resulting angles produced by the perpendicular height are ϕ_1 and ϕ_2, respectively, the following relationship holds:

$$\phi_0 = \phi_1 + \phi_2. \tag{2}$$

Although we quantify the *external* elbow angle in the HS-AFM analyses, the *internal* angle is more convenient for the theoretical derivation. The external angle θ_0 and the internal angle ϕ_0 are related by:

$$\phi_0 = \pi - \theta_0. \tag{3}$$

Geometrically, the height h_0 can be expressed as:

$$h_0 = L_1 \cos\phi_1 = L_2 \cos\phi_2 \tag{4}$$

By applying the addition theorem to decompose the third term, we obtain:

$$L_1 \cos\phi_1 = L_2 \left(\cos\phi_0 \cos\phi_1 + \sin\phi_0 \sin\phi_1\right) \tag{5}$$

Solving this expression for ϕ_1 yields:

$$\phi_1 = \tan^{-1}\left(\frac{\frac{\alpha}{1-\alpha} - \cos\phi_0}{\sin\phi_0}\right) \tag{6}$$

$$\phi_2 = \phi_0 - \phi_1 \tag{7}$$

Furthermore, a_1 and a_2 are given by:

$$\begin{aligned} a_1 &= L_1 \sin(\phi_1), \\ a_2 &= L_2 \sin(\phi_2). \end{aligned} \tag{8}$$

Next, we consider the case in which the control points are placed manually. Let Δh represent the maximum positional error in locating the elbow, and let $\Delta\phi$ denote the resulting angular error. Geometrically, the elbow angle is then expressed as:

$$\phi_1 + \Delta\phi_1 = \tan^{-1}\left(\frac{a_1}{h_0 + \Delta h}\right), \tag{9}$$

$$\phi_2 + \Delta\phi_2 = \tan^{-1}\left(\frac{a_2}{h_0 + \Delta h}\right), \tag{10}$$

By combining these results, we obtain the following equation:

$$\begin{aligned} \Delta\theta &= -\Delta\phi_1 - \Delta\phi_2 \\ &= \phi_0 - \tan^{-1}\left(\frac{\sin\phi_1}{\cos\phi_1 + \frac{\Delta h}{\alpha L_0}}\right) - \tan^{-1}\left(\frac{\sin\phi_2}{\cos\phi_2 + \frac{\Delta h}{(1-\alpha)L_0}}\right). \end{aligned} \tag{11}$$

When we substituted L_0=30 nm and α=0.4 (the elbow position of Smc6) into this equation and plotted the result, we found that the error strongly depends on Δh. The error also shows a slight decreasing trend as θ_0 increases. Since the full width at half maximum (FWHM) of SMC arms in AFM images is approximately 8 nm, we consider Δh=1−2 nm to be a reasonable estimate. Therefore, the angular error is estimated to be approximately 8°–16°.

Aside from theoretical estimations, we also measured the arm angles using the same dataset by three independent analysts to evaluate measurement error (Supplementary Fig. 8d). From these data, we calculated the mean standard deviations, which were 4.7° for Smc5 and 6.4° for Smc6. Accordingly, twice the standard deviation, corresponding to the ~95% confidence range, was approximately 13° for both Smc5 and Smc6, consistent with the theoretical estimation described above. Although arm-angle measurements involve a certain degree of error, the magnitude of this error was similar for both Smc5 (which associates with Nse2) and Smc6. Therefore, we conclude that arm angles are measured with comparable accuracy for both SMC arms. These results have been incorporated into Supplementary Fig. 8.

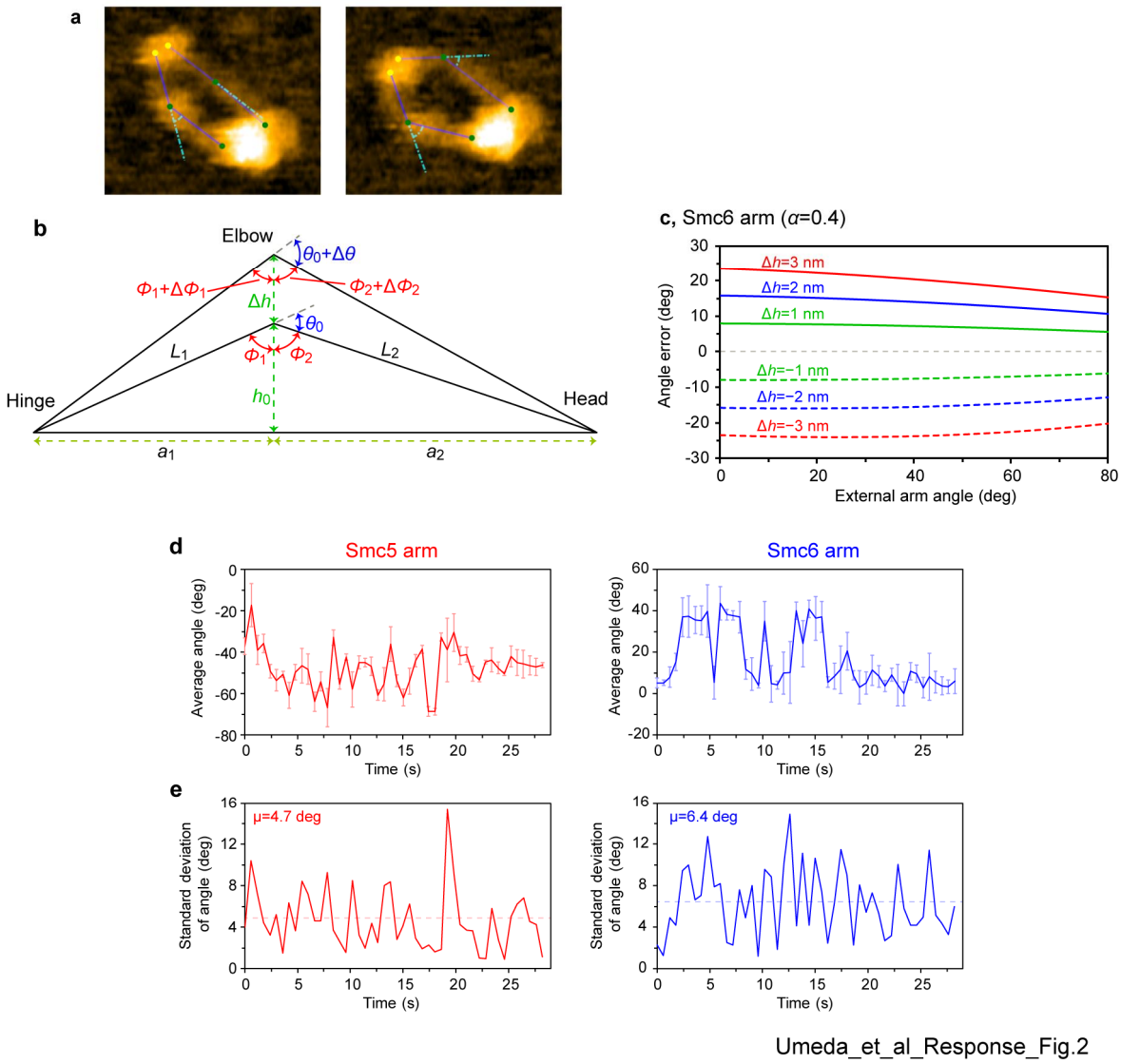

Response Figure 2| Quantification of the bending angles at the Smc5/6 arms.

a, Measurement of SMC arm bending angles. For each SMC arm, a two-segment ridge line was placed connecting the hinge to the head. The yellow and green dots indicate the control points corresponding to the hinge domain and other domains, respectively. The bending angle was then measured at the junction between the two segments (see Methods).

b, Theoretical framework for calculating errors in SMC arm angle measurements (see below for details).

c, Estimation of angular errors using the framework shown in (b) under different parameter settings.

d, Real-time traces of SMC elbow angles measured by three independent analysts using the same dataset of 100 frames. The graph shows the average elbow angles measured by the three analysts (authors of this study). Error bars represent the standard deviation.

e, The standard deviation at each time points was plotted. The means standard deviation (μ, dash-lines) for the Smc5 and Smc6 are 4.7 and 6.4 degrees, respectively.

• For the analysis in Figure 6, where were the points on the DNA for the contour placed, where the complex was overlaid to the DNA itself? How robust is the analysis to such a placement?

Thank you for this insightful comment. In the analysis shown in Fig. 6, control points were manually placed along the DNA contour, and a spline-interpolated line was generated. Based on the contour information obtained from this spline, we calculated the radius of gyration (R_g). The actual DNA trajectory was obscured in regions where Smc5/6 was bound. In such cases, we extrapolated the contour line across the bound region by extending the DNA shape before and after the protein. As the reviewer correctly pointed out, some degree of error may arise in regions where Smc5/6 is bound. To assess the magnitude of this error, we performed an additional test in which two different sets of control-point placements were manually defined across the Smc5/6-bound region in Fig. 6. For the Twisted state in particular, we inspected multiple frames and generated alternative spline reconstructions for comparison. As shown in Response Fig. 3, the estimated errors in R_g were approximately 0.7%, 0.4%, and 3% for Bound1, Bound2 (bridge), and Twisted, respectively. Therefore, the measurement error in the R_g analysis appears to be as small as ~3% and does not affect our conclusions. These results have been incorporated into the main text (lines 325–326) and added as Supplementary Fig. 16.

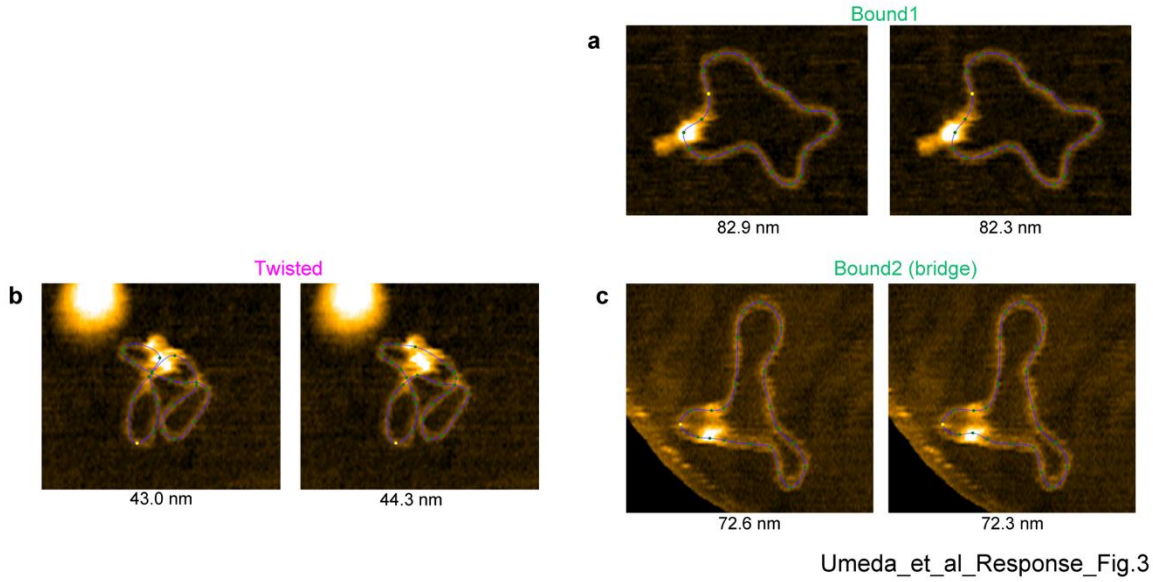

Response Figure 3| Radius of gyration (Rg) analysis of DNA using different line trajectories in the Smc5/6-bound region.

a–c, Comparison of R_g values calculated using two different line trajectories in the Smc5/6-bound region from the same HS-AFM images. The Bound1 (a), Bound2 (bridge) (b), and Twisted (c) conformations shown in Fig. 6a are analysed. To calculate the R_g of Smc5/6-bound DNA, control points were manually placed along the DNA contour, and a spline-interpolated line was generated. The actual DNA trajectory became ambiguous in regions bound by Smc5/6, particularly in the Twisted species. To estimate this uncertainty, R_g was calculated using two different sets of control-point placements in the Smc5/6-bound regions, yielding an estimated error of ~3%.

Finally, in the material and methods, it is stated that: “To quantitatively measure the molecular size and DNA length, we implemented a function to compensate for the nonlinearity and tip-position dependence of the XY piezo scanner (this will be published elsewhere)” Such a statement makes it hard to evaluate the appropriateness of the procedure (likely correct given the expertise of the authors, but still unverifiable at this point). Perhaps the author could explain the concept behind it without going into too much detail or, vice versa, briefly show any data in support of the correctness without revealing details?

Thank you for this insightful comment. We provide a detailed explanation below. In high-speed AFM, the probe is scanned using a piezo scanner. Calibration is typically performed under the assumption that the piezo expands and contracts linearly with the applied voltage. However, nonlinearities are present in actual HS-AFM scanning, and we found that distances estimated from AFM images can contain errors as large as 20–30%. We recently revealed that the primary sources of distance error can be classified into four major categories (Response Fig. 4):

1. Tip position (offset voltage) dependency
2. Scan size nonlinearity
3. Scan wave hysteresis
4. Scan frequency

The control software developed in our laboratory implements feedforward correction for these effects, enabling the distance error to be reduced to below 1%. The details of this work have been published in the following paper.

Kenichi Umeda (1st) and Noriyuki Kodera:

“Feedforward compensation of piezo nonlinearity for high-precision high-speed atomic force microscopy”,

Scientific Reports, **in press** (2026). DOI: 10.1038/s41598-026-55176-7

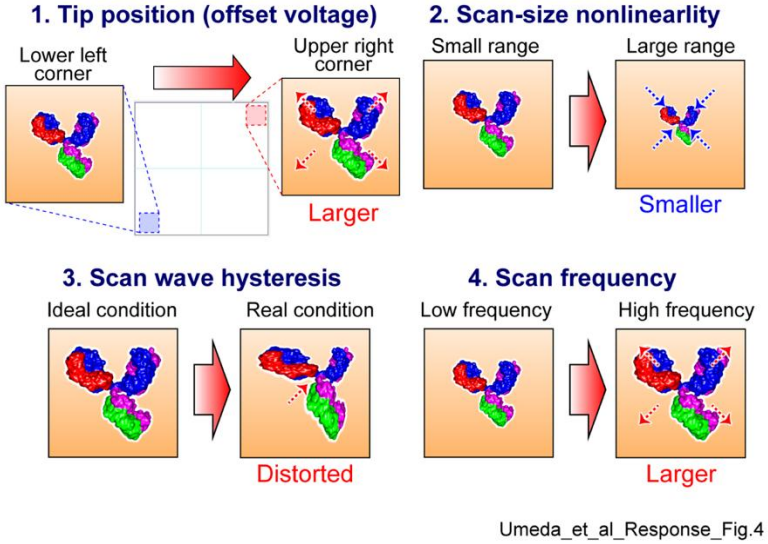

Response Figure 4| Summary schematics illustrating four types of nonlinearities in piezo scanners that affect AFM imaging. A monoclonal antibody (PDB: 1IGT) is shown as a schematic model, with its apparent size and shape exaggerated for clarity.

Response to Reviewer #2: In this study, the authors used high-speed atomic force microscopy (HS-AFM) to visualise the structural dynamics of budding yeast Smc5/6 complexes at submolecular resolution. Within the Smc5/6 hexamer, they predominantly observed two types of extended architectures—the I-form and the O-form—whose prevalence correlated with the ATP-binding state of the complex. They also found that Nse2 stabilises the extended conformation of Smc5/6 by preventing elbow bending within the SMC arms, in contrast to the flexible elbow dynamics characteristic of cohesin and condensin. Based on these findings, the authors propose that Smc5/6 compacts DNA through a DNA–DNA tethering mechanism. More broadly, they suggest that DNA–DNA tethering may be a conserved biochemical property among SMC complexes, complementing their ability to extrude DNA loops. The manuscript is well written and easy to follow. The resolution the authors achieved in their HS-AFM experiments is impressive. Overall, this work adds valuable insights to research on SMC complex activities.

General comments:

We thank reviewer 2 for their positive comments on our study and for acknowledging its significance. They pointed out several valid concerns about the role of Nse2 in the structural dynamics and DNA-binding state of Smc5/6 at the ATPase heads (Head-O/I states). We also appreciate the many useful suggestions for resolving these issues.

In order to assess the effect of Nse2 directly, we purified Smc5/6 lacking Nse2 (the pentamer; see Response Fig. 5a) and performed comparative analyses with the wild-type (WT) complex. The results are summarized below:

1. In Smc5/6 lacking Nse2, a small population of molecules adopted a B-form, which was not observed in the WT complex.
2. In the B-form, the arm–arm distance is greater than in the O-form.
3. In the absence of Nse2, the angular distribution of the SMC arms is broader than in the wild type (WT), indicating increased conformational flexibility of the arms.

Together, these results suggest that Nse2 constrains the Smc5 arm angle within a defined range and thereby reduces the conformational freedom of the Smc5/6 complex.

Following the reviewer's suggestion, we also performed additional experiments to further investigate the DNA-binding state of Smc5/6. The results of these experiments are consistent with and further support our conclusions. Details are provided below.

Comments:

Nse2 dissociation: My main concern relates to the interpretation of Nse2 dissociation. I am not entirely convinced that the results presented in this section (Fig. 3, Supplementary Fig. 4, and Supplementary Movie 3) sufficiently support such a strong conclusion. I would recommend validating the proposed complex dynamics by performing additional biophysical experiments specifically examining Nse2 association and dissociation.

We thank Reviewer 2 for this insightful and important comment. We understand Reviewer 2's concern that our conclusion that Nse2 maintains the Smc5 arm at a defined angle and thereby contributes to stabilization of the Smc5/6 structure is based on analyses of Smc5/6 complexes in which Nse2 may have partially dissociated.

Upon revisiting the original manuscript, we realized that several descriptions in the original manuscript were insufficiently detailed regarding the experimental conditions and may therefore have led to misunderstanding. We sincerely regret this lack of clarity. In particular, the role of salt concentration in the different HS-AFM experiments was not described with sufficient clarity.

An important consideration in HS-AFM observations of Smc5/6 is the salt concentration of the imaging buffer. As described in the original manuscript, a high-salt buffer (300 mM KOAc) prevented disruption of the Smc5/6 complex and enabled stable imaging on mica over time. Under these conditions, Smc5/6 predominantly adopted I- or O-forms, and no B-form with bent arms was observed.

In contrast, as shown in the original Fig. 3d, HS-AFM imaging was performed under low-salt conditions (75 mM KOAc) in the case of experiments examining Nse2 dissociation. Under these conditions, Nse2 dissociated from Smc5/6 at a certain frequency. Notably, B-form formation was observed only when Nse2 had dissociated. Therefore, in the original manuscript, this observation was used as one line of evidence supporting the conclusion that Nse2 stabilizes the Smc5 arm angle. However, the B-form appears to represent a transient state that occurs during eventual disruption of the Smc5/6 complex, and not all Nse2-dissociated molecules adopted the B-form. The original description could be interpreted as implying that B-form formation always occurs upon Nse2 dissociation, which was misleading.

In the analysis shown in the original Supplementary Fig. 4, we reported that the angle distribution of the Smc5 arm exhibited a single peak when Nse2 was present, whereas the Smc6 arm showed a broader, bimodal distribution. Although noted in the figure legend, this analysis was also performed using data obtained under low-salt conditions to highlight differences between Smc5 and Smc6 dynamics. However, we acknowledge that quantification should be performed using data obtained under high-salt buffer conditions. Presenting results from low-salt conditions may have led to potentially misleading interpretations, and we regret this oversight.

Based on these considerations, we sought to directly assess the effect of Nse2 on Smc5/6 structure by newly purifying Smc5/6 lacking Nse2 (the pentamer, –Nse2, see Response Fig. 5a) and performing HS-AFM imaging under the same high-salt conditions used for WT (the hexamer, +Nse2). Under high-salt conditions, the complex remained intact even in the absence of Nse2, allowing long-term imaging (Response Fig. 5b). We first quantified the occurrence frequencies of different SMC conformations. Although the majority of molecules adopted I- and O-forms, the B-form was also observed at a low frequency of approximately 3% (Response Fig. 5c). As noted above, this B-form was not observed in the WT complex.

We further tracked individual pentamer molecules (–Nse2) over time to measure their arm–arm distances. Although I- and O-form molecules frequently transitioned between the two conformations (i.e., I-to-O and O-to-I transitions), the B-form tended to remain in a bent conformation. Quantification of arm–arm distances revealed two clear peaks at 7 nm and 17 nm, corresponding to the I- and O-forms, respectively (Response Fig. 5d). In addition, a distinct peak at 33.5 nm was observed for the B-form, representing a larger arm–arm distance. These results suggest that Nse2 suppresses the range of arm motion and that, in its absence, the arms can adopt sharply bent

conformations. However, because the B-form appears at low frequency even in the pentamer, it likely represents a transient and relatively unstable structural state rather than a stable conformation comparable to the I- and O-forms.

To further investigate the mechanical effects of Nse2 on arm structure, we quantified the elbow angles of Smc5 and Smc6 for each molecule (Response Fig. 5e). In this analysis, molecules were oriented with the hinge positioned upward and the head downward. Arm angles were defined as negative when oriented to the left and positive when oriented to the right, and the distributions were analysed accordingly (see schematics on the left in Response Fig. 5e). In the presence of Nse2, the Smc5 arm showed a peak at negative angles below 0°, whereas the Smc6 arm exhibited a broader distribution. The standard deviation of Smc6 angles was approximately two-fold greater than that of Smc5. In Smc5/6 lacking Nse2 (pentamer), both Smc5 and Smc6 showed an approximately 2–3-fold increase in standard deviation compared with the Nse2-bound Smc5/6 complex. These results suggest that Nse2 restricts the elbow angle of the Smc5 arm within a defined range, thereby reducing structural flexibility. Indeed, previous electron microscopy studies have reported that, in the absence of Nse2, Smc5/6 adopts a shorter and more compact conformation.

As pointed out by the reviewer, HS-AFM observations are performed under two-dimensional confinement because molecules are adsorbed onto a mica surface. This constraint may influence structural dynamics. In a three-dimensional environment, the arms may exhibit greater freedom of motion, and conformations corresponding to the B-form observed here may occur more frequently, even in the presence of Nse2.

Based on these analyses, we have revised the original Fig. 3d to include results from Smc5/6 lacking Nse2 (the pentamer) and updated the text accordingly (new Fig. 3d–f and Supplementary Fig. 7, Lines 175–198 and 362–368). We have also revised the section title to: "**Observation of Smc5/6 lacking Nse2.**"

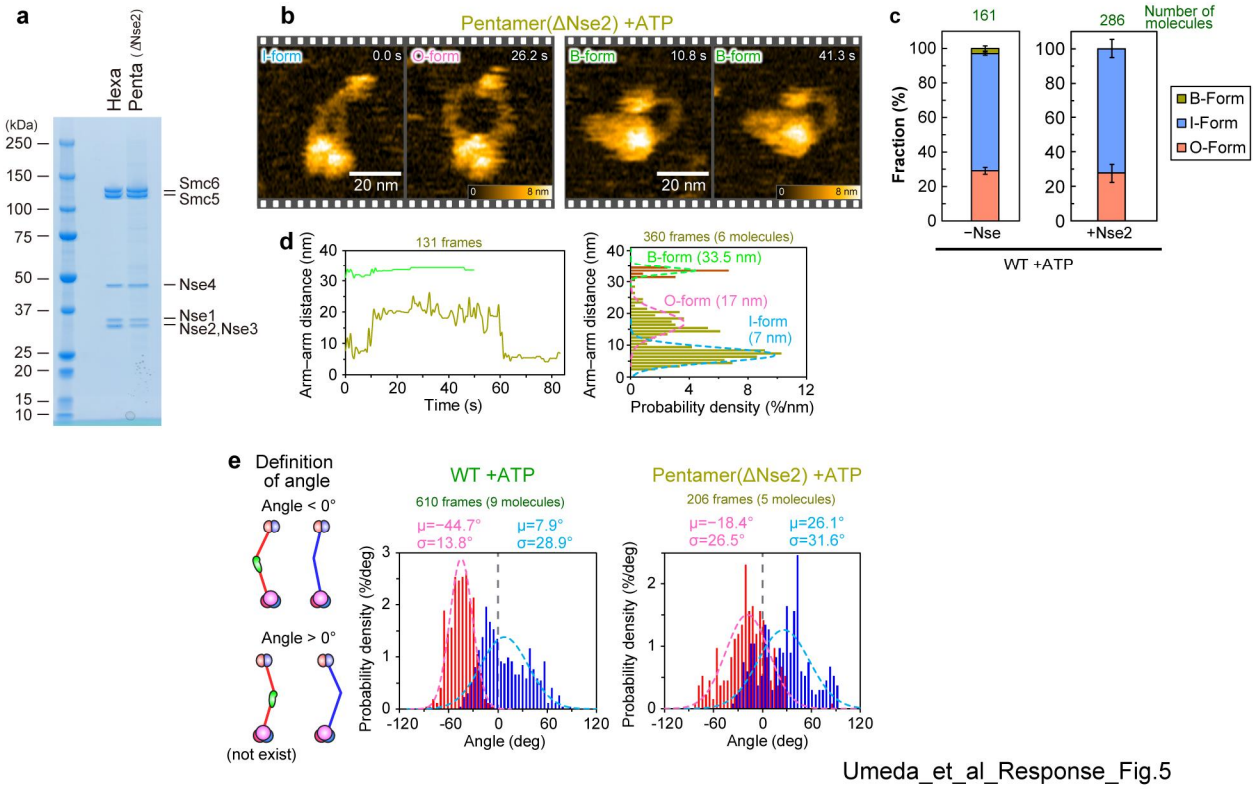

Umeda_et_al_Response_Fig.5

Response Figure 5| Purification and HS-AFM observation of Smc5/6 lacking Nse2 (pentamer).

a, Purified Smc5/6 pentamer along with the hexamer were analysed by SDS-PAGE followed by CBB staining.

b, Successive HS-AFM images of the pentamer lacking Nse2 (related to Supplementary Movie 3). Representative I/O- and B-form molecules are shown. Scan area, 120 × 120 nm^2 at 200 × 100 $pixels^2$, cropped to 62 × 65 nm^2. Imaging rate, 0.63 s per frame.

c, Abundance ratios of different conformations calculated from the individual pentamer molecules (obtained from three independent experiments), where error bars represent s.d. The data for the hexamer (+Nse2) from Fig. 1d is shown for comparison.

d, Distributions of arm-to-arm distances extracted from successive HS-AFM images under each condition. The total number of frames and analysed molecules are indicated in each chart. The values in brackets next to each component label represent the fitted mean values of the Gaussian distributions.

e, Quantification of SMC arm bending angles. The red and blue histograms represent the probability density distributions of the bending angles of the Smc5 and Smc6 arms, respectively. The mean angle values and their standard deviations are shown as μ and σ above each peak.

Lines 278-280: Did authors try to carry out this experiment with the wt Smc5/6 and ATP analogues? Especially in the context of experiment of DNA recovery (Fig. 6e).

Thank you for this valuable suggestion. We attempted HS-AFM imaging in the presence of the ATP analogue ADP–AlFx. However, under these conditions the molecular features of Smc5/6 became unclear, and reliable imaging was not possible. Therefore, we used the EQ mutants to analyse the ATP-bound state of Smc5/6. In bulk biochemical assays, ADP–AlFx supported DNA loading (Fig. 4b) and DNA–DNA tethering (Supplementary Fig. 18a) of wild-type Smc5/6 to a similar extent as observed for the EQ mutant.

LINE 101: Does DNA binding shift the equilibrium toward the O-form? Given that DNA has been shown to stimulate ATP hydrolysis, it would be valuable to assess whether it also stabilizes the "O-form," in which the ATPase heads of SMC5/6 are engaged. This could potentially be tested using a short dsDNA oligonucleotide, similar to the approach used for the cryo-EM structure of SMC5/6 bound to DNA. It may additionally be informative to test oligos containing an ss/ds junction, to examine SMC5/6 conformations relevant to structures arising during replication stress or double-strand break repair.

We thank Reviewer 2 for this insightful suggestion. We observed the Smc5/6 hexamer on mica in the presence of a >100-fold excess of 20-bp dsDNA and ATP (we confirmed binding of the Smc5/6 hexamer to 20-bp DNA by EMSA, as shown in Response Fig. 6a). We observed an approximately 10% increase in the O-form fraction compared with the condition without short dsDNA (Response Fig. 6b,c).

As Reviewer 2 pointed out, the reported cryo-EM structure shows DNA clamped between the ATPase head domains and Nse1/3, accompanied by opening of the SMC arms (Yu Y. et al., PNAS, 119, e2202799119, 2022). The short-DNA experiment is consistent with this model, in that the O-form fraction increases when DNA is bound in a similar manner.

However, we also found that the large amount of short dsDNA added in this assay extensively adsorbs onto

the mica surface (see ReviewerOnly_Video01.mov). Therefore, we cannot exclude the possibility that nearby adsorbed DNA indirectly influences the observed Smc5/6 conformations, or that Smc5/6 binds DNA at the engaged ATPase heads as shown in the cryo-EM structure. It is technically challenging to suppress non-specific DNA adsorption on mica while preserving Smc5/6 adsorption. Thus, while Reviewer 2's comment was highly valuable, we were unable to fully resolve this point. We have added this explanation to the main text (Lines 112–118) and Supplementary Fig. 4.

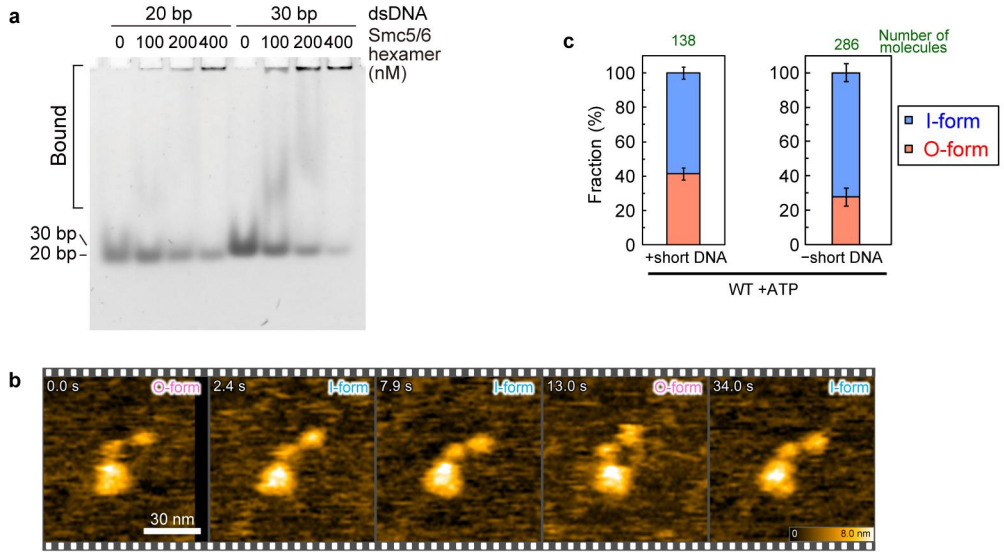

Umeda_et_al_Response_Fig.6

Response Figure 6| Effect of Short DNA on the Conformation of Smc5/6

a, Binding of Smc5/6 to short double-stranded DNA (20 bp and 30 bp) was analysed using an electrophoretic mobility shift assay (EMSA).

b, HS-AFM imaging of Smc5/6 hexamers in the presence of an excess amount of 20 bp short DNA. Scan area, 120 × 120 nm^2 at 80 × 80 $pixels^2$, cropped to 102 ×102 nm^2. Imaging rate, 0.34 s per frame.

c, Abundance ratios of I- and O-forms in the presence of 20 bp DNA calculated from individual molecules (obtained from three independent experiments), where error bars represent s.d.

LINE 167: For SMC5, the centre of mass of the Nse2 subunit could reasonably be used to define a point for angle measurement along the coiled coil. For SMC6, however, this is more difficult as there is no equivalent density at the coil midpoint. Because the angle determination is based on manually selected points rather than a statistical framework (as stated in the Methods, Line 780: "three control points were manually placed"), I would caution against reporting numerical angle values, as they may appear somewhat arbitrary.

(Please also see the response to Reviewer 1 for comment 2 stating with "For the analysis in Figure 3", as this

point was also raised by Reviewer 1).

Thank you for this valuable suggestion. As Reviewer 2 pointed out, we used Nse2 to define the control point on the Smc5 arm. For the Smc6 arm, we applied the following criterion to place the control point on the curved region of the arm. As shown in Fig. 2, our simulation suggested that the O-form conformation can be induced by bending the Smc6 arm at Joint 1 (the elbow), which is located at an approximately 40:60 ratio between the hinge–elbow and elbow–head segments. We therefore placed the control point according to this ratio. In some frames, the Smc6 arm appeared nearly straight and its curvature was not clearly discernible. In such cases, the control point on the Smc6 arm was still positioned using the same 40:60 ratio between the hinge–elbow and elbow–head segments.

We also measured the arm angles of both Smc5 and Smc6 using the same dataset (100 frames) by three independent analysts (authors of this study). The results showed mean standard deviations of 4.7° for Smc5 and 6.4° for Smc6. Accordingly, twice the standard deviation, corresponding to the ~95% error range, was approximately 13°. We acknowledge that the angle measurements contain some error; however, the magnitude of the error is similar for Smc5 and Smc6. Therefore, we conclude that both SMC arms are measured with comparable accuracy. These results have been included in Supplementary Fig. 8.

LINE 171: The final step shown in Figure 3d is described as a “broken” complex with a split hinge; however, in both the figure and Supplementary Movie 3, it is hard to discriminate 2 hinge domains. Could the final step of figure 3d be interpreted as an “I-form” without the Nse2 subunit? Additional observations could be made on Supplementary Movie 3. For example, in the frames 16.4s – 16.7s -17s there seems to be a rapid detachment of the ATPase heads, followed by a rebinding. After that the conformation of the of the complex results less clear. To support the interpretation of the proposed “B-structure” or “broken complex,” it would strengthen the manuscript if additional representative examples were included.

Thank you for this comment. We agree that the original presentation could be misleading and may have given the impression that the observed structure was an I-form. The original Fig. 3 and Supplementary Movie 3 had been edited specifically to highlight the formation of the B-form. Separation of the two SMC arms was visible in later time points that were not included in the original manuscript, as shown in the third frame in Response Fig. 7.

As mentioned above regarding Nse2 dissociation, we have now performed additional HS-AFM experiments using the Smc5/6 pentamer lacking Nse2 and obtained more quantitative results regarding the role of Nse2 in Smc5/6 conformation. Therefore, we would like to replace the original Fig. 3d and Supplementary Movie 3 with data obtained under high-salt buffer conditions, which are now presented in the new Fig. 3d–f.

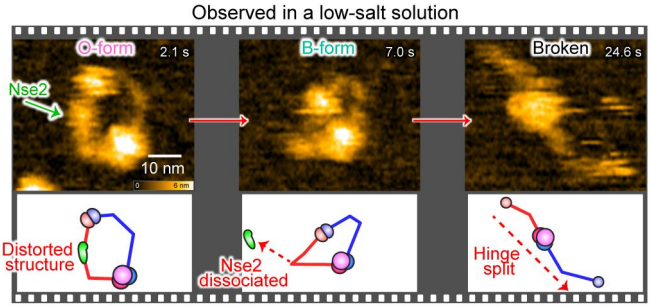

Umeda_et_al_Response_Fig.7

Response Figure 7| Successive HS-AFM images of wild-type hexamer molecules undergoing Nse2 dissociation, observed in a buffer solution with a low KOAc concentration (75 mM).

LINE 184: The linear DNA retention data (Fig. S5a) suggest that the EQ mutant may in fact retain DNA more effectively than the WT protein. Maybe this could reflect DNA binding in the clamp conformation, without transition in other regions of the SMC5/6 complex. This seems to be confirmed in Supplementary movie S4 and S5. In movie S4, the WT protein seem to interact with the DNA at the hinge domain, (probably after a first entrapment of the DNA between the heads) and seems to be jumping around the DNA quite often (second 50.9, second 105.8), which explains why upon linearization the DNA is lost. Instead, the EQ mutant is stuck in one position, and the DNA is entrapped between the heads domain in the clamp conformation. Could the authors elaborate the discussion considering these points?

We appreciate this astute observation. We agree with this interpretation and have now added a discussion that the Head–O configuration frequently observed in the EQ mutant may also represent DNA held in the clamp conformation. As shown below, in additional experiments prompted by another insightful suggestion from Reviewer 2 (regarding Lines 317), we found that the EQ mutant can capture DNA within the kleisin subunit even under conditions where the ATPase heads are pre-engaged prior to DNA addition. A previous biochemical study has demonstrated that Smc5/6 topologically holds DNA in a segment-capture state, in which Smc5/6 binds DNA in the clamp conformation while entrapping it within the kleisin compartment (Taschner M. et al., NSMB, 30, 619–628, 2023). We therefore speculate that the EQ mutant in the Head–O state represents an altered form of segment capture. In this state, the EQ mutant topologically entraps DNA while also gripping it strongly by sandwiching a DNA segment between the ATPase heads and Nse1–Nse3. This discussion has been added to the Discussion section (Lines 399–403).

SUPPLEMENTARY FIGURE 7a: It would be informative if the authors could measure the head–hinge distances in the four displayed snapshots and comment on whether this correlates with the proposed conformational states. More generally, the first two images classified as Head-I may also be explainable as Head-O viewed with the O-ring oriented perpendicular rather than parallel to the imaging plane. Similar considerations could apply to Figure 5b–c.

Thank you for this valuable suggestion. We quantified the head–hinge distances in both the original Fig. 5 and

Supplementary Fig. S7a. As shown in Response Fig. 8 below, we did not detect a significant difference in head–hinge distances between the O- and I-forms in the Fig. 5 dataset. Similar results were also obtained from Supplementary Fig. S7a. These results indicate that O- and I-forms cannot be reliably distinguished based on head–hinge distance alone.

In addition, we quantified the head–hinge distances of Smc5/6 molecules adsorbed on mica. However, we did not observe any significant difference in head–hinge distance between the I- and O-forms, which were defined by their respective arm–arm distances of 8.5 and 18 nm (see Fig. 3b). Therefore, it is sometimes difficult to determine whether a given state represents a true I-form or an O-form transiently captured in an I-form–like configuration within a single frame. Accordingly, in such cases where this distinction is ambiguous, for the classification shown in Fig. 5e, we inspected multiple consecutive frames before and after each frame and classified each molecule into the three categories based on temporal behaviour. These points have been described in the revised main text (Lines 272–274).

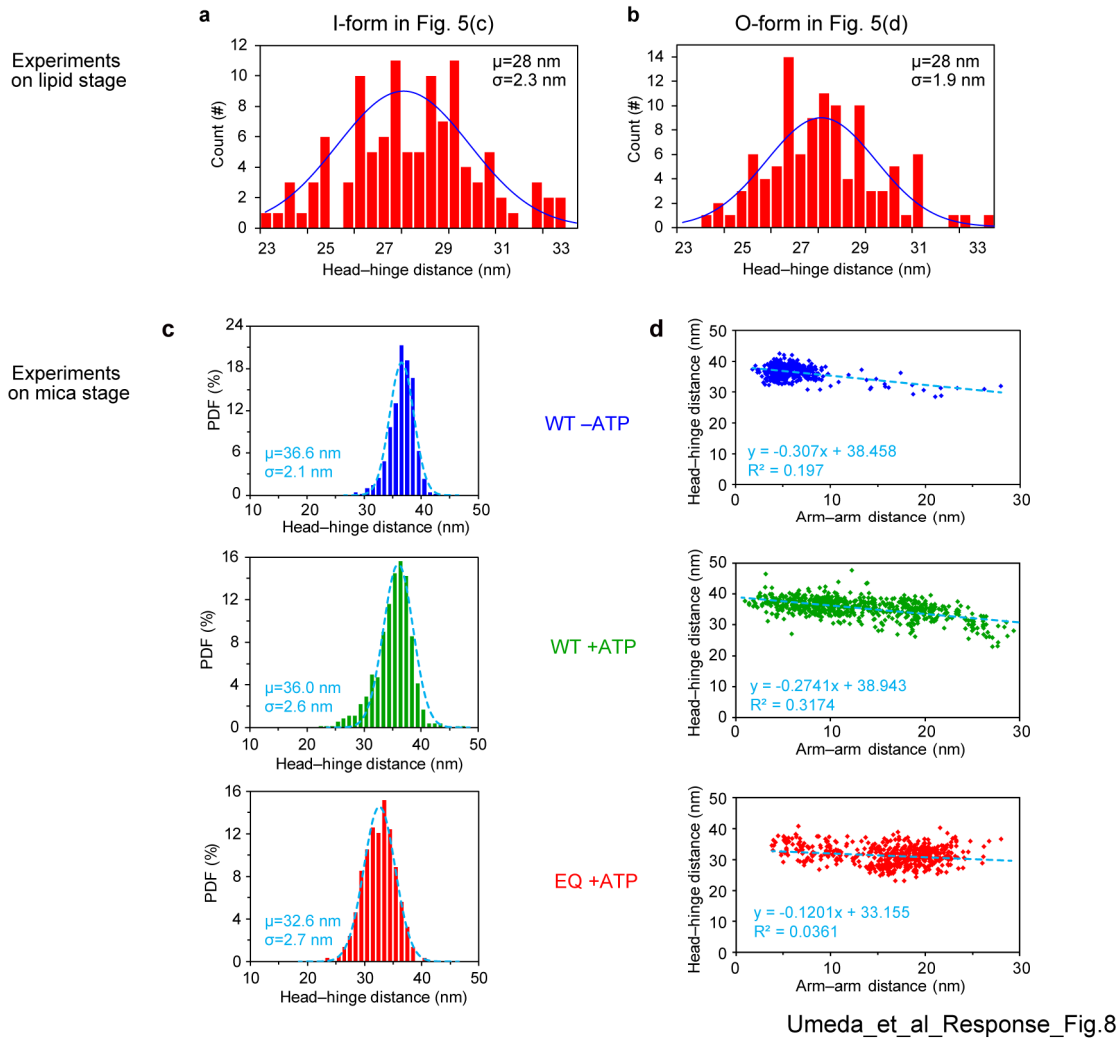

Response Figure 8| Quantification of the head–hinge distance.

a, b, Statistical analysis of the head-to-hinge distances for the I-form (a) and the O-form (b), as observed in Fig. 5c and Fig. 5d. In the graph, μ and σ represent the mean and the standard deviation, respectively. The fitting

parameters of the Gaussian curves are shown in the graphs.

c, Distribution of head-to-hinge distances extracted from the data in Fig. 3c. The mean (μ) and standard deviation (σ) obtained by Gaussian fitting are shown in the graph.

d, Correlation between the arm-to-arm distance and the head-to-hinge distance. The linear regression equation and the R^2 value obtained by linear fitting are shown in the graph.

LINE 317: "We speculate that Smc5/6 initially entraps DNA within the kleisin compartment and subsequently transfers it to the SMC compartment upon ATP hydrolysis" The authors propose that DNA is initially captured inside the kleisin compartment and later transferred into the SMC compartment upon ATP hydrolysis. However, available cryo-EM structures of SMC complexes—including SMC5/6 (Yu et al., PNAS, 2022)—show DNA occupying the SMC compartment even in ATP-engaged but hydrolysis-defective states. While AFM clearly demonstrates Head-O binding near the ATPase domains, it remains unclear whether the DNA lies inside or outside the SMC ring. A potential experiment to test this model would be to pre-engage the heads using the SMC5/6 EQ mutant with ATP or ADP-BeF_3, then introduce DNA afterward and visualize using AFM. If the DNA can be captured by a pre-closed complex, it may indeed indicate initial kleisin-only entrapment. https://www.pnas.org/doi/10.1073/pnas.2202799119

We appreciate this insightful suggestion. We tested whether Smc5/6 can capture DNA even when the ATPase heads are already engaged upon ATP binding. As suggested by Reviewer 2, we first incubated the EQ mutant with ATP to induce head engagement prior to DNA addition.

First, in the bulk loading assay, similar levels of DNA recovery were observed regardless of the order in which ATP, DNA, and Smc5/6 were added (Response Fig. 9a). We then performed HS-AFM imaging of the resulting mixtures adsorbed onto the lipid stage. As shown in Response Fig. 9b,c, consistent with the bulk loading assay, no substantial differences were observed in either DNA-binding efficiency or the population of DNA-bound structures (Head-O, Head-I, or Hinge-O/I) compared with those under the standard conditions (without ATP pre-incubation). These observations strongly support the conclusion that Smc5/6 entraps DNA within the kleisin compartment in its ATP-bound form. These results have now been incorporated into the main text (Lines 279–290) and added as Supplementary Fig. 13.

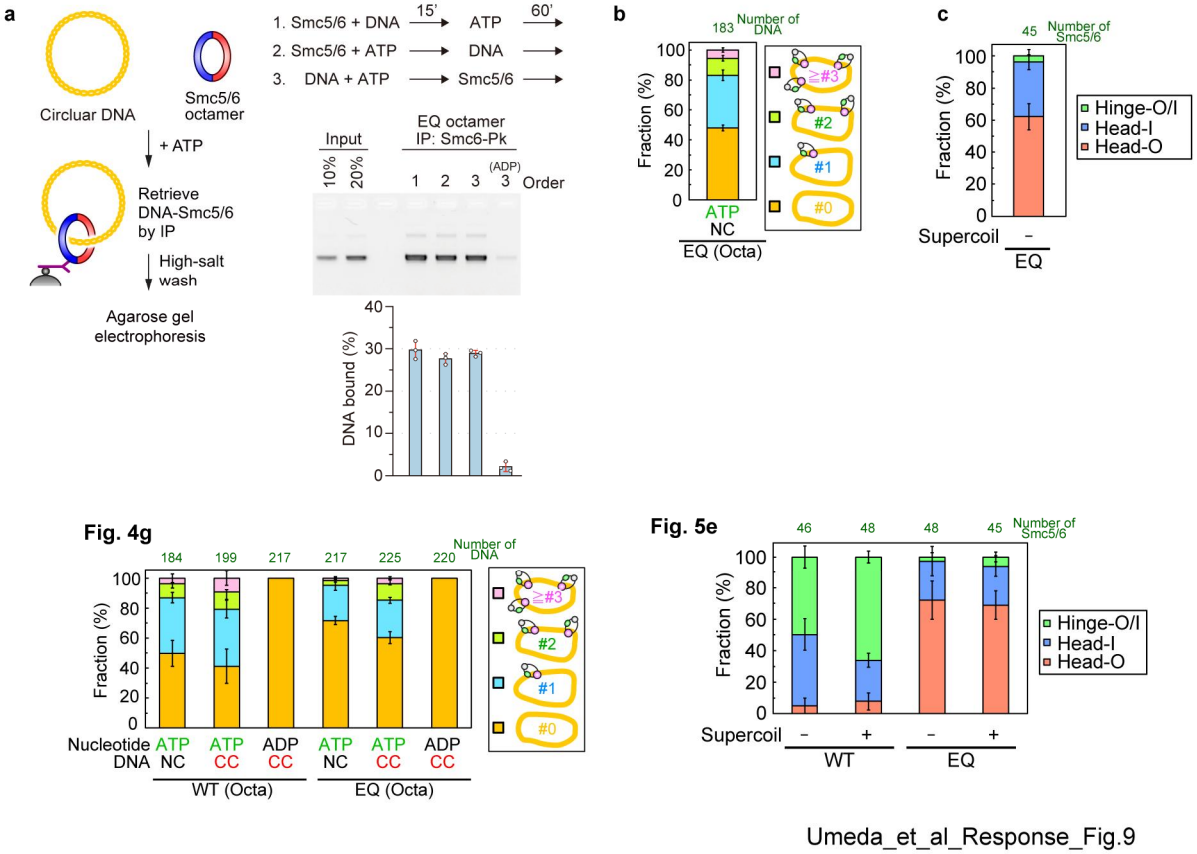

Umeda_et_al_Response_Fig.9

Response Figure 9| Topological DNA loading of ATP-prebound EQ-Smc5/6 to examine the loading scheme.

a, Schematic and gel images of the EQ-Smc5/6 pre-incubated with ATP and then mixed with DNA to examine topological DNA loading scheme.

b, Quantification of Smc5/6 molecules bound to DNA observed using HS-AFM experiments on lipid membrane (from three independent experiments), with error bars representing s.d.

c, Abundance ratios of DNA-bound Smc5/6 conformations (from three independent experiments). Error bars represent s.d.

For comparison, the results obtained from samples loaded without controlling the order of mixing (Fig. 4g and Fig. 5e) are also shown.

Minor comments:

Line 132: Fig.2e in red.

This has been corrected, Thank you.

Lines 221-222 : The sentence is not clear. Please restructure it to improve readability.

We have revised the sentence to improve readability. The updated text is now shown in Lines 256-259.

Lines 290-292 :I suggest explicitly highlighting that DNA-tethering activity requires ATP binding but not ATP hydrolysis.

We have revised the text to explicitly highlight that DNA-tethering activity requires ATP binding but not ATP

hydrolysis. The updated text is now shown in Line 348-349.

Line 299 :The word mediate is used twice ("…Smc5/6 mediates mediate DNA–DNA tethering…").

This has been corrected, Thank you.

Response to Reviewer #3: In this manuscript, the authors use high-speed AFM (HS-AFM) to visualise budding yeast Smc5/6. They present data showing two conformations for the Smc5/6 hexamer, characterised by I- and O-shaped complexes and track transitions between these two states demonstrating through the use of an ATP hydrolysis mutant (EQ) that ATP binding causes the transition to O shape. They also investigate the ability of Smc5/6 to engage DNA and classify interactions based on whether they occur through different regions of the complex (i.e. heads and hinge). The authors argue that these interactions represent different stages of topological loading, meaning that the DNA is caught within the SMC-kleisin tripartite architecture. They used biochemical bulk assays that include high salt washes as a main argument for topological loading. Finally, they also propose DNA:DNA tethering by Smc5/6 and DNA compaction, using a combination of AFM and bulk assays. The technical execution of AFM and the image quality are very good, and the lipid-supported system is a valuable advance. The authors clearly observed the predicted structure of Smc5/6 and demonstrate the I and O states and convincingly link the ATP binding in the transition between the two states. They also show that on DNA SMC head regions readily interact with DNA upon ATP binding, using the EQ complex. However, they argue that they are observing topological loading on DNA, making this point a key claim of their work. Unfortunately, this topological binding is not supported by the data. In fact the AFM data strongly argues against it. In summary, although the HS-AFM imaging is of high technical quality and the conformational transitions between I and O states are convincingly documented, the manuscript ultimately demonstrates only that Smc5/6 interacts with DNA mainly through its ATP-head regions upon ATP binding, an interaction already well supported by prior structural work. The central claim that these observations represent topological loading is not backed by the data presented, and several aspects instead argue against such an interpretation. As a result, the manuscript risks introducing misconceptions into the field rather than clarifying Smc5/6 mechanism. I cannot support publication of this work unless the authors unequivocally demonstrate, through appropriate crosslinking-based assays, that the complexes they visualise are indeed topologically loaded.

General comments:

We thank Reviewer 3 for the thoughtful and critical comments on our study. The reviewer raised concerns regarding our interpretation of the HS-AFM observations as evidence of topological DNA loading by Smc5/6 and suggested a protein crosslinking approach to further verify this conclusion.

We agree that covalent ring closure through site-specific crosslinking is a powerful biochemical method for investigating topological DNA entrapment by SMC complexes, including Smc5/6. However, the primary focus of this study is to investigate the structural dynamics of Smc5/6 on DNA in its native, non-crosslinked state. Therefore, although informative, a crosslinking-based approach would not directly address the central question examined in this work (please see our detailed response below).

To further validate our interpretation of topological Smc5/6 loading observed by HS-AFM, we performed several additional experiments. In summary, we found that:

1. Using an Smc5/6 hexamer lacking Nse5-Nse6, we demonstrated that DNA loading by Smc5/6 depends on Nse5–Nse6, consistent with the results obtained from both HS-AFM observations and bulk biochemical assays.
2. We also confirmed that the apparent jumping behaviour of Smc5/6, involving dissociation from and re-association with DNA, hardly occurred under our HS-AFM conditions.
3. Smc5/6 mediates stable DNA-DNA tethering, particularly when multiple Smc5/6 molecules are bound to the same DNA substrate.

Taken together, these additional experiments further support our interpretation that the HS-AFM observations reflect topological loading of Smc5/6 onto DNA.

Specific comments

1. One of the central claims of the manuscript is that Smc5/6 topologically loads onto DNA and that HS-AFM directly visualises this binding with DNA within either the kleisin or SMC compartments. Salt-resistant binding does not necessarily imply topological entrapment. The authors rely heavily on high-salt washes (Fig. 4b) to infer topological capture. Numerous studies on cohesin have shown that salt resistance alone is insufficient to distinguish between topological and strong non-topological binding, for example when DNA is in the gripping state (not topologically loaded). Importantly, topological entrapment has been demonstrated in previous studies through crosslinking of the interfaces of the SMC-kleisin tripartite ring, something that is not done here. Crosslinking experiments demonstrated that topological entrapment is strongly driven by ATP-hydrolysis. In contrast, DNA interactions that survive high-salt washes can still occur in the absence of ATP hydrolysis. Here the authors show that their EQ hydrolysis mutant resists high-salt washes therefore in this experimental conditions the authors cannot conclude that topological loading has been achieved.

We thank Reviewer 3 for this insightful suggestion. We performed additional experiments to address the topological loading of Smc5/6 in our reconstitution system. As pointed out by Reviewer 3, topological loading strictly depends on Nse5–Nse6 (Taschner M. et al., NSMB, 30, 619–628, 2023). Therefore, we tested the Nse5–Nse6 dependency in our bulk loading assay using a Smc5/6 hexamer (lacking Nse5–Nse6) together with separately purified Nse5–Nse6. The Smc5/6 hexamer alone did not show DNA loading regardless of ATP. In contrast, DNA loading of the Smc5/6 hexamer was substantially enhanced by the addition of Nse5–Nse6 (Response Fig. 10a,b). This loading was ATP-dependent, as Nse5–Nse6 did not promote DNA loading of Smc5/6 in the absence of ATP (Response Fig. 10a,b). The same Nse5–Nse6 and ATP dependency was also observed for the EQ mutant (Response Fig. 10a,b). These results indicate that, under our experimental conditions, efficient DNA loading occurs only in the presence of the reported factors required for topological loading (Nse5–Nse6 and ATP).

We also performed HS-AFM observations using the Smc5/6 hexamer (lacking Nse5–Nse6). The hexamer complex was first incubated with DNA in the presence of ATP, and the reaction mixture was then visualised by HS-AFM using a lipid stage. Among 76 DNA molecules analysed, none showed Smc5/6 binding (Response Fig. 10c). In stark contrast, approximately 50% of DNA molecules were bound by at least one Smc5/6 complex when the Smc5/6 octamer containing Nse5–Nse6 was used. This Nse5–Nse6 dependency observed by HS-AFM is fully

consistent with the bulk loading assay, demonstrating that Smc5/6–DNA binding is only detectable under conditions that support topological loading. These results have been incorporated into the main text (Lines 207–210 and 240–241), Fig. 4g, and added as Supplementary Fig. 10a.

As noted by Reviewer 3, ATP-bound states of SMC complexes exhibit salt-resistant DNA binding. Although the structures differ slightly, in both the segment-capture state of Smc5/6 and the gripping state of cohesin, DNA has been reported to be trapped within the kleisin compartment (Higashi T. et al., Mol. Cell, 79, 917–933, 2020). In these ATP-bound states, a DNA segment is sandwiched between the ATPase heads and non-SMC subunits through multiple DNA-binding motifs, which likely contributes to salt resistance. Taken together, these additional experiments indicate that topological DNA loading by Smc5/6 is successfully reconstituted in our system.

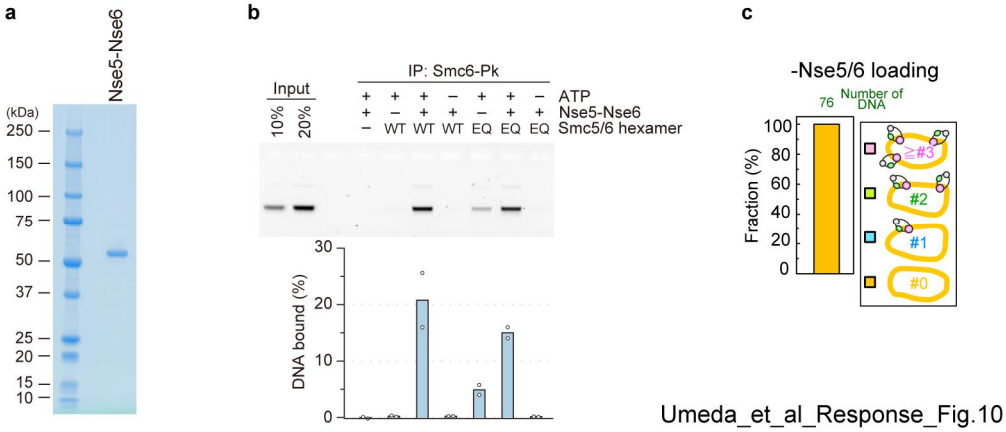

Response Figure 10| Nse5/6 is required for Smc5/6 DNA loading, supporting topological engagement.

a, Purification of the Nse5/6 heterodimer. Purified Nse5/6 was analysed by SDS-PAGE followed by CBB staining.

b, Agarose gel analysis of the DNA loading experiment using the Smc5/6 hexamer and separately purified Nse5-Nse6. Efficient DNA recovery was seen only when Nse5-Nse6 was added in the presence of ATP.

c, Analysis of the binding frequency of Smc5/6 molecules in HS-AFM imaging when loading was performed with the Smc5/6 hexamer lacking Nse5-Nse6.

In addition, the AFM data clearly contradicts topological entrapment. The authors show that wild-type complexes freely transition between I and O conformations and they argue that are these complexes are topologically loaded in their AFM images, however the complexes can be observed in the movies to jump from one side of the DNA to another, something impossible if DNA were threaded inside a closed ring. Please refer to Movie S4 and S6 (left pannel for WT complexes; loaded complexes detach and reattach at distal/different positions along the DNA contour). There is also a degree of confusion when interpretating of the imaging data. In Fig. 4e the authors state that Smc5/6 is engaged with DNA through a hinge-mediated, topologically trapped intermediate. However, the still image they present in this figure corresponds to a frame from Movie S4, and the full movie shows a completely different behaviour: again the complex argued to be topologically loaded seems to jump from one side of the DNA to the other in a single frame during the movie. Such a discontinuous relocation is incompatible with any form of

topological entrapment. Similar situation is shown in Fig. 5b, and Movie S6. In addition, the authors overinterpret the meaning of small linear movement of the complex along DNA, claiming that it is evidence for a topologically entrapped state. Linear displacement on DNA can also arise from simple one-dimensional diffusion of a protein bound non-topologically, particularly under the high-salt conditions used in the assay where electrostatic screening reduces non-specific sticking and facilitates sliding. Diffusive motion therefore cannot be taken as an indicator of ring-closure or topological capture.

Thank you for this valuable suggestion. Reviewer 3 expressed concern that the behaviours of Smc5/6 observed by HS-AFM, such as "jumping" and apparent "dissociation and re-association," may not reflect topological DNA entrapment but instead non-topological electrostatic interactions. We conclude that such dissociation and re-association events are highly unlikely under our HS-AFM conditions, based on the following additional experiments.

If Smc5/6 repeatedly dissociates from and re-associates with DNA, *de novo* loading events should be observable during HS-AFM imaging. Therefore, we tested whether free Smc5/6 in the imaging buffer can bind to pre-adsorbed DNA on the lipid membrane stage. We first immobilized circular DNA substrates on the lipid stage, followed by buffer exchange to remove unbound DNA. We then applied Smc5/6 with ATP and performed HS-AFM imaging. Note that excess Smc5/6 and DNA were used to facilitate potential binding in this experiment. Nonetheless, we did not observe Smc5/6 binding to DNA under this order of addition (Response Fig. 11a and ReviewerOnly_Video02.mov).

This result indicates that, under our current HS-AFM conditions, freely diffusing Smc5/6 in the imaging buffer cannot stably bind to DNA immobilized on the lipid stage, even in the presence of ATP. This is likely because DNA is weakly adsorbed to the lipid membrane, which suppresses *de novo* DNA loading via electrostatic interactions and subsequent topological entrapment by freely diffusing Smc5/6. Thus, the long-distance displacement events of DNA-bound Smc5/6 observed in Supplementary Movie S6c are unlikely to reflect dissociation and re-association events.

In contrast, as described above, DNA-bound Smc5/6 was observed only when Smc5/6 was pre-incubated with DNA in the presence of Nse5–Nse6 and ATP, both of which are required for topological loading of Smc5/6.

Why were apparent "jump" events observed? In our lipid membrane stage system, the surface of the lipid membrane is weakly positively charged, and DNA segments are therefore weakly adsorbed to the membrane through electrostatic interactions. As a result, a DNA segment can transiently detach from the membrane surface. Because Smc5/6 exhibits little or no interaction with the lipid membrane itself, when the DNA segment carrying Smc5/6 lifts off the surface, the complex can undergo rapid lateral diffusion. If this motion occurs within a time interval shorter than the HS-AFM frame acquisition time, it can appear as an instantaneous long-range displacement between consecutive frames. Indeed, during an apparent "jump" event (50.9–51.9 s), the DNA segment between the start and end positions of the jump appears transiently distorted in Supplementary Movie S6. Importantly, even in such cases, Smc5/6 remains continuously associated with DNA rather than dissociating from it.

In addition, we occasionally observed dissociation of Smc5/6 from DNA even when Smc5/6 had been pre-loaded onto DNA in solution prior to HS-AFM imaging (i.e., the standard condition used in this study). As

shown in Response Fig. 11b and ReviewerOnly_Video03.mov, upon dissociation, Smc5/6 did not re-associate with DNA but instead rapidly disappeared from the field of view. Importantly, such dissociation events were extremely rare. We therefore prefer not to include this observation in the main manuscript, as it may give the misleading impression that dissociation occurs frequently. We provide it here solely for the reviewer's consideration.

Taken together, these results indicate that only Smc5/6 molecules loaded onto DNA in an Nse5–Nse6- and ATP-dependent manner are stably observed in our HS-AFM experiments (Fig. 5b-d), and that dissociated Smc5/6 is unlikely to rebind to the same DNA. Therefore, the dynamics of Smc5/6 observed in this study are most consistent with topological DNA loading. These results have been described in Lines 247–251 and added as Supplementary Fig. 11.

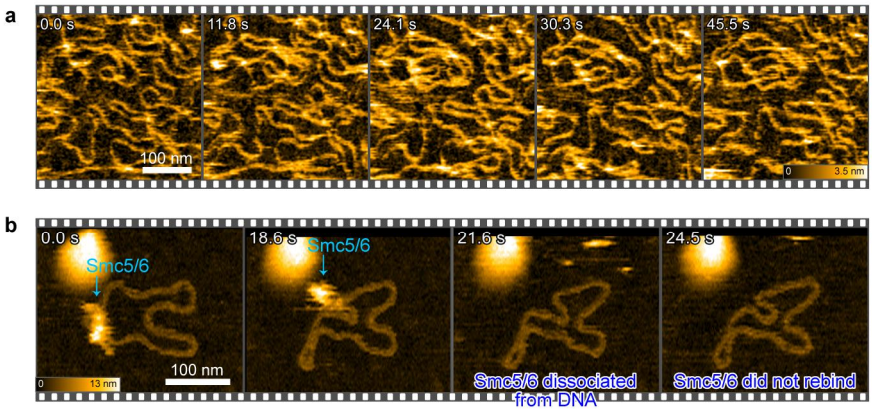

Umeda_et_al_Response_Fig.11

Response Figure 11| Free Smc5/6 molecule does not bind to DNA pre-adsorbed on the lipid membrane.
a, HS-AFM images from an experiment in which DNA was first adsorbed onto the lipid membrane and Smc5/6 was subsequently added to the observation chamber. Only DNA is observed, indicating that the Smc5/6 complexes do not adsorb to the surface under these conditions.
b, HS-AFM images showing a rare dissociation event in which a Smc5/6 complex detached from DNA after apparent rupture of its ring structure. Following dissociation, the Smc5/6 complex did not re-bind to the DNA, but instead rapidly disappeared from the field of view, further supporting that free Smc5/6 molecules do not bind to DNA pre-adsorbed on the lipid membrane under our imaging conditions.

The manuscript does not provide adequate biochemical or AFM evidence to support its central claim of topological loading. Definitive assignment of DNA to either the kleisin or SMC compartment requires conditional closure of specific ring interfaces by crosslinking. Cross-linking of the Smc–kleisin interfaces has long been the gold-standard biochemical test for topological entrapment, and including these experiments here would allow the authors to distinguish unequivocally between topological and non-topological associations. Without such controls, the current data remain insufficient to sustain the claims made.

We thank the reviewer for this important suggestion. We agree that compartment-specific crosslinking has been widely used as a powerful biochemical approach to investigate DNA entrapment by SMC complexes. However, the objective of the present study is to directly visualise the DNA-binding behaviour and structural configuration of

individual Smc5/6 complexes under native conditions using HS-AFM. In this context, compartment-specific crosslinking experiments would provide biochemical information regarding DNA entrapment, but would not directly address the structural states and DNA-binding configurations visualised in the present work. Furthermore, conventional crosslinking-based entrapment assays rely on biochemical analysis following chemical crosslinking and denaturing treatment, whereas the conclusions of the present study are based on direct observation of individual Smc5/6–DNA complexes in their native state. We therefore consider these approaches to provide different types of information regarding Smc5/6–DNA interactions. To further strengthen our interpretation, we have performed additional experiments as mentioned above, which provide further support for topological entrapment.

2. A further concern relates to the authors' claim of DNA:DNA tethering activity based on AFM data. The events they interpret as "tethering" appear to be extremely transient, often limited to a single or a few frames, and, as presented, are indistinguishable from stochastic contacts between two nearby DNA segments containing complexes. Short-lived proximity or brief co-movement is not sufficient evidence of a genuinely stable bridging interaction, particularly in an AFM setting. To substantiate a tethering mechanism, the authors would need to demonstrate persistent and mechanically meaningful interactions events that remain stable across multiple frames or show coordinated movement of both DNA arms in a way that cannot be explained by random diffusion. Without such evidence, the interpretation of these very brief contacts as "tethers" is not convincing.

We have observed the DNA compaction products over time under HS-AFM. Notably, over 80% of "Twisted" species that were bound by more than two Smc5/6 maintained stable DNA-DNA tethering after multiple-frame scanning ranging from 60-120 frames (1-2 min). Please see Response Fig. 12a and Supplementary Movie 7 as examples of DNA-DNA tethering. We also observed DNA-bound Smc5/6 that were moving in concerted with two DNA strands, with appearance of small DNA loops (Response Fig. 12b,c). As reviewer pointed out, we also observed short-lived DNA bridging that we have categorized as "Bound 2" in Fig 6a3 especially when single Smc5/6 bound to DNA. In contrast to these cases, DNA molecules bound by multiple Smc5/6 molecules retained stable DNA twisting or DNA-DNA tethering over time during HS-AFM scanning. These results demonstrate that Smc5/6 mediate DNA compaction through DNA-DNA tethering when multiple Smc5/6 bind to DNA. These results have been incorporated into the main text (lines 334-338) and added as Supplementary Fig. 18 and Supplementary Movie 7.

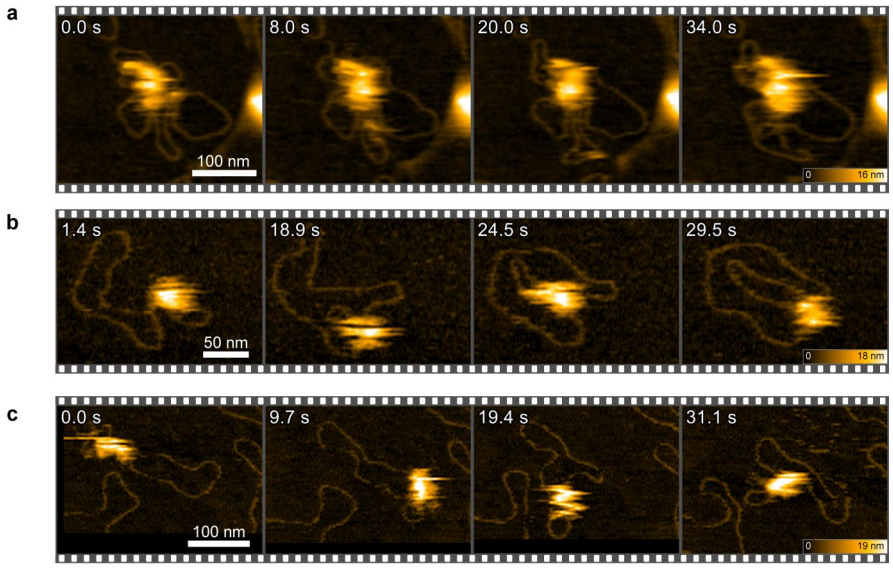

Umeda_et_al_Response_Fig.12

Response Figure 12| Stabilization of the Twist Structure by Smc5/6 oligomer

a, Successive HS-AFM images of twisted DNA species bound by multiple Smc5/6 molecules forming a cluster. Smc5/6 exhibited persistent interactions with DNA across multiple consecutive frames (Supplementary Movie 7a).

b,c, Smc5/6 clusters tethered two DNA strands and displayed coordinated movement. Two representative examples are shown (Supplementary Movie 7b,c).

Other comments

1. It is well-established that Smc5/6 hinge has a preference for ssDNA rather than dsDNA. The authors mention that Smc5/6 associates strongly with nicked plasmids. Since a nicked plasmid, even if mostly double-stranded, inevitably carries local ssDNA regions, could these intereactions represent engagement with ssDNA?

We performed HS-AFM experiment using both nicked and intact, covalently closed circular DNA. Although we mainly presented the nicked DNA results in the figures because the absence of torsional stress makes the images easier to interpret, the DNA-binding efficiency of Smc5/6 did not differ dramatically between the two substrates; supercoil DNA showed a slightly higher binding efficiency (Fig. 4g). Thus, no clear effect attributable to DNA nicks was detected in our experiments. Smc5/6 has been reported to function in homologous recombination and DNA replication, chromosomal processes in which ssDNA is an important intermediate. As Reviewer 3 pointed out, the hinge domain of Smc5/6 has been reported to have high binding affinity to ssDNA (Alt A., et al, Nat Commun, 14011, 2017). Although the DNA binding and dynamics of Smc5/6 to such non-B form DNA are somewhat outside the focus of this study, they represent an important avenue for future investigation.

The authors need to compare the behaviour of hexameric versus octameric Smc5/6 assemblies on DNA by AFM and contrast their binding behavior. Nse5/6 is required for bona fide topological loading, and therefore any claim of topological entrapment made from octamer-based assays must be contrasted with

the behaviour of the hexameric core. Such a comparison may reveal mechanistic differences that could be attributed to conditions where topological binding can (or cannot) occur.

Thanks for this insightful comment. Evaluation of Nse5-Nse6 contribution on DNA loading in our system is indeed a critical point that was missing from our original submission. As mentioned in Specific comment 1, we performed DNA loading reaction with Smc5/6 hexamer in the presence of ATP, which was subject to HS-AFM observation. DNA-bound Smc5/6 was not detected using the hexamer complex (please see Response Fig. 10). This result strongly supports the conclusion that DNA-bound Smc5/6 observed in this study is in a topologically bound state.

Reviewer #1 (Remarks to the Author):

I thank the authors for their thorough revisions and responses to my comments. The authors have satisfactorily addressed all of my concerns, including those related to the robustness and description of the quantitative analyses. The manuscript provides valuable insights into the conformational dynamics of the Smc5/6 complex and its interactions with DNA through high-speed AFM. The study advances our understanding of ATP-dependent conformational changes, alternative DNA-binding modes, and DNA compaction by Smc5/6. I am satisfied with the revised manuscript and consider it suitable for publication in its current form.

We would like to thank the referee for the critical reading of our revised manuscript, and for recommending it for publication in Nature Communications.

Reviewer #2 (Remarks to the Author):

the authors have clarified the issues raised in the previous version of the manuscript and improved the clarity of the manuscript

We would like to thank the referee for the critical reading of our revised manuscript, and for acknowledging its improvement and significance.

Reviewer #3 (Remarks to the Author):

I thank the authors for their thorough and carefully considered response to my concerns. The additional experiments have strengthened the manuscript in several important respects, and I acknowledge the significant effort made to address my criticisms. However, I maintain several reservations that I outline below.

We would like to thank the referee for critically reading our revised manuscript and for acknowledging the improvements made. In response to Reviewer 3's suggestions, we have added the following points to the Discussion, as detailed below.

Topological loading, Nse5/6 dependency

The new data demonstrating that the Smc5/6 hexamer lacking Nse5–Nse6 fails to load onto DNA in both bulk assays and HS-AFM imaging (0 of 76 DNA molecules bound) is the most convincing addition to the manuscript. Since Nse5–Nse6 dependence is an established hallmark of topological loading, this result substantially strengthens the authors' interpretation. I am largely satisfied by this response, and consider this the most important advance over the original submission.

We thank the reviewer for pointing out the dependence on Nse5–Nse6. We also appreciate the

reviewer's acknowledgement that the additional experiments performed in response to this comment improved our assessment of the specificity of Smc5/6 binding to DNA.

Jumping behaviour and apparent dissociation/re-association

The authors' explanation, that apparent jumping events reflect transient detachment of DNA from the lipid membrane followed by rapid lateral diffusion within a single frame acquisition time is plausible. The supporting experiment showing that freely diffusing Smc5/6 in the imaging buffer cannot bind to pre-adsorbed DNA further argues against simple rebinding as an explanation for these events. I accept that the authors have provided a reasonable account of the jumping artefact. However, I note that this explanation was developed post hoc in response to my criticism, and the evidence for it remains indirect. The authors infer that DNA briefly lifts off the membrane based on apparent distortion of the DNA contour during jump events, which is suggestive but not conclusive. A more direct demonstration (for example by systematically varying lipid membrane composition to modulate DNA adsorption strength and showing that jump frequency correlates accordingly) would have been more convincing. I acknowledge this may be beyond the scope of the current revision, and I do not insist on it as a condition for publication, but I would ask the authors to present this explanation clearly as an inference rather than an established fact in the revised manuscript.

Thank you for this comment. Regarding the possibility that Smc5/6 dissociates from and subsequently rebinds to DNA, we believe that the additional experiments demonstrate that such events are unlikely, as also acknowledged by Reviewer 3. We also understand the need to explain the transient lifting of DNA. However, because this explanation requires a relatively lengthy description and is somewhat tangential to the main text, we considered it more appropriate to present our interpretation separately. We therefore added a reference to this explanation at the relevant position in the main text (lines 242) and described our interpretation of the abrupt displacement of Smc5/6 along DNA in Supplementary Note 1, based on the explanation provided in our previous response letter.

"**Supplementary Note 1:** DNA-bound Smc5/6 occasionally underwent relatively long-range translocation within only a few frames, as shown in Supplementary Movie S6. We interpret these abrupt displacements as follows. In our lipid-membrane stage system, the membrane surface is weakly positively charged, allowing DNA segments to adsorb weakly through electrostatic interactions. Consequently, a DNA segment can transiently detach from the membrane surface. Because Smc5/6 exhibits little or no interaction with the lipid membrane itself, when the DNA segment carrying Smc5/6 lifts off the surface, the complex can undergo rapid lateral diffusion. If this motion occurs within a time interval shorter than the HS-AFM frame acquisition time, it can appear as an instantaneous long-range displacement between

consecutive frames. Indeed, during the long-distance displacement observed between 50.9 and 51.9 s, the DNA segment spanning the initial and final positions of Smc5/6 appeared transiently distorted in Supplementary Movie S6. These observations are consistent with Smc5/6 remaining continuously associated with the DNA throughout this event rather than dissociating and rebinding."

Crosslinking-based ring closure assays

I appreciate the authors' position that compartment-specific crosslinking experiments address a conceptually different question from what their HS-AFM study examines. Nevertheless, I remain of the view that making a strong claim of topological entrapment without the gold-standard biochemical validation leaves the manuscript vulnerable. The Nse5/6 dependency data provides important indirect support, but it demonstrates a requirement for a factor known to be involved in topological loading, not topological loading itself. I will not insist on crosslinking experiments as an absolute condition for publication given the new supporting data. However, I strongly urge the authors to explicitly acknowledge in the Discussion that direct biochemical proof of ring closure (through interface-specific crosslinking) has not been performed in this study, and that their interpretation of topological loading is based on convergent indirect evidence. This is an honest and important qualification that readers deserve, and it is consistent with rigorous scientific reporting.

We recognize that crosslinking assays are important for directly demonstrating the topological association of SMC complexes with DNA. We have therefore added the following statement to the Discussion (lines 404).

"Although our HS-AFM observations directly visualize the dynamic behavior of DNA-bound Smc5/6 and the dependence on Nse5–Nse6 provides additional support, our interpretation of topological loading is based on convergent but indirect evidence rather than direct biochemical proof of DNA entrapment within a closed Smc5/6 ring. Nevertheless, HS-AFM complements these biochemical approaches by providing insight into the structural dynamics of reconstituted DNA-bound Smc5/6 without requiring covalent ring closure."

DNA-DNA tethering

The new data showing that over 80% of twisted species bound by multiple Smc5/6 molecules maintain stable DNA-DNA tethering over 60–120 consecutive frames (1–2 minutes) substantially addresses my concern about the transient nature of the observed

bridging events. The examples of coordinated movement of two DNA strands with apparent loop formation are also more convincing than what was presented originally. I am satisfied that this claim is now better supported, though I note that the mechanistic interpretation of how Smc5/6 mediates this tethering (whether through simultaneous engagement of two DNA segments by a single ring or through oligomerisation) remains speculative and should be presented as such.

Although DNA–DNA tethering appears to be more stable when mediated by multiple Smc5/6 complexes, as the reviewer correctly pointed out, we have not yet been able to determine the precise molecular architecture responsible for this stabilization. We have clarified this limitation by adding the following statement to the Discussion (lines 424).

“Although the structural resolution of our HS-AFM images was insufficient to determine how Smc5/6 clusters establish a stable compacted DNA state, the combined HS-AFM and biochemical results suggest that Smc5/6 promotes DNA compaction through a DNA–DNA tethering mechanism.”

In summary, the authors have made meaningful progress in addressing my concerns. The Nse5/6 dependency experiments represent a genuine advance and substantially shift the evidential basis for topological loading. The remaining gap (absence of direct crosslinking-based ring closure evidence) should be acknowledged explicitly as a limitation rather than left implicit. Subject to this acknowledgement being incorporated clearly into the Discussion, and to the jumping artefact explanation being presented as an inference rather than a conclusion, I am prepared to support publication.

We would again like to thank the reviewer for acknowledging the progress made in our revision. We believe that addressing the comments above has further strengthened the manuscript and improved its overall rigor. We sincerely appreciate the reviewer’s thoughtful and constructive feedback.